UCRL 3580
c.8

UNIVERSITY OF CALIFORNIA

Radiation Laboratory

TWO-WEEK LOAN COPY

This is a Library Circulating Copy which may be borrowed for two weeks. For a personal retention copy, call Tech. Info. Division, Ext. 5545

BERKELEY, CALIFORNIA

DISCLAIMER

This document was prepared as an account of work sponsored by the United States Government. While this document is believed to contain correct information, neither the United States Government nor any agency thereof, nor the Regents of the University of California, nor any of their employees, makes any warranty, express or implied, or assumes any legal responsibility for the accuracy, completeness, or usefulness of any information, apparatus, product, or process disclosed, or represents that its use would not infringe privately owned rights. Reference herein to any specific commercial product, process, or service by its trade name, trademark, manufacturer, or otherwise, does not necessarily constitute or imply its endorsement, recommendation, or favoring by the United States Government or any agency thereof, or the Regents of the University of California. The views and opinions of authors expressed herein do not necessarily state or reflect those of the United States Government or any agency thereof or the Regents of the University of California.

UCRL-3580

UNIVERSITY OF CALIFORNIA
Radiation Laboratory
Berkeley, California

Contract No. W-7405-eng-48

ANALYSIS OF BEVATRON TAU MESONS

Roy Phillip Haddock

(Thesis)

November 5, 1956

Printed for the U.S. Atomic Energy Commission

ANALYSIS OF BEVATRON TAU MESONS

Contents

Abstract 4

I. Introduction

A. Statement of the Problem 5

B. Historical Background 5

C. Experimental Method 11

II. Experimental Arrangement

A. K Beam 12

B. Stacks 16

III. Microscope Work

A. Scanning by Track-Following 17

B. Measurement of Pion Ranges

1. Method 17

2. Errors 17

a. Air Gaps 17

b. Range Straggle and Reading Errors 19

c. Alignment 19

d. Stage-Stop Error 19

e. Distortion and Rub-Off Errors 19

f. Range Shortening 19

C. Measurement of Direction Cosines

1. Method 20

2. Errors 20

a. Error in Angle 21

b. Error in ρ 21

c. Error in z 21

d. Effect of Multiple Scattering 21

e. Effect of Direction-Cosine-Errors on Coplanarity 22

f. Effect of Direction-Cosine-Errors on Momentum Balance 22

Contents (cont.)

IV. Pion Energy and Mass of Tau Meson
A. Method 26
B. Discussion 26
C. Results 27
V. Spin and Parity . . . . . .
A. Design of Experiment
1. Selection of a Bias-free Sample 30
2. Coplanarity and Momentum Balance 30
3. Statistics and Sample Size 30
B. Discussion 33
C. Results 40
VI. Polarization
A. Method 41
B. Discussion and Results 41
VII. Summary of Results 46
Acknowledgments 47
Appendices
A. Direction-Cosine Errors
1. Derivation of direction-cosine errors due to measurement errors and multiple Coulomb scattering 48
2. Effect of Direction-Cosine Errors on Coplanarity . 50
3. Effect of Direction-Cosine and Energy Errors on Momentum Balance 51
B. Humidity Error 53
C. Effect of Increasing the Interaction Radius 54
D. Table of Original Data 57
References 66

ANALYSIS OF BEVATRON TAU MESONS

Roy Phillip Haddock

Radiation Laboratory
University of California
Berkeley, California

November 5, 1956

ABSTRACT

One hundred and seventy-seven τ^+ mesons, obtained from large nuclear emulsion stacks exposed to the Kerth-Stork K^+ beam at the Bevatron and located by systematic track-following, are analyzed for (a) Q value of the tau decay, (b) tau spin and parity, (c) possible polarization effects. A Q of 75.13 ± .20 Mev is obtained. The corresponding tau mass is 966.5 ± .74 m_e. A relativistic treatment of the Dalitz analysis was used to assign the tau spin-parity. The observed energy and angle distributions do not agree with any of the cases compatible with the decay of the tau into two pions whereas the cases (0 -), (2 -), (3 +) were about equally probable and no final conclusion concerning the spin was possible. In this connection no polarization effect was found, which does not contradict a pseudoscalar meson.

I. INTRODUCTION

A. Statement of the Problem

Until recently the methods employed to collect information about the "τ" meson have been inadequate in the sense that the accumulated number of taus was small and strongly biased, and measurements of the tau characteristics were subject to significant uncertainties. Improved techniques and experimental conditions now make it possible to surmount these difficulties. It is the purpose of this experiment to collect a significant number of accurately measured bias-free taus. This sample will then be analyzed for the energy release of the tau decay, spin-parity of the tau, and possible polarization effects.

B. Historical Background

Soon after the perfection of photographic emulsion sensitive to minumum ionizing particles, Brown[1] and co-workers discovered and correctly interpreted an event in which a singly charged particle of approximately 900 m_e decayed at rest into three coplanar charged pions. This event, the first τ meson, was not, however, the first evidence for heavy unstable mesons. Rochester and Butler,[2] in 1947, reported the observation of two cloud-chamber events which they interpreted as the decay of a neutral particle and the decay of a charged particle of mass considerably greater than that of the pion. Since then, many different decay modes of a particle of mass about that of the τ meson, which are positively and negatively charged[3-7] as well as neutral,[6,7,8] have been observed. This particle is called the K meson.

Paramount interest in K-meson physics centers about the question: Is the K meson a single particle with many different modes of decay or is it several distinct particles of about the same mass? What must be done to answer this question is perfectly clear. One must

determine the mass, spin-parity, electric and magnetic moments, and production and interaction cross sections for the various modes.

Dalitz has suggested that an investigation of the angular distribution of all pions and of the energy spectrum of π^- mesons emitted in the decay of the τ meson,

$$\tau^{\pm} \rightarrow \pi^{\pm} + \pi^{+} + \pi^{-} + 75 \text{ Mev}$$
$$\rightarrow \pi^{\pm} + 2\pi^{0} + 85 \text{ Mev},$$

might reveal its spin and parity.[9] If the tau spin-parity resulting from this type of investigation were consistent with that of the decay of the meson into 2 pions,

$$\theta^{+} \rightarrow \pi^{+} + \pi^{0} + 220 \text{ Mev},$$
$$\theta^{0} \rightarrow \pi^{+} + \pi^{-} + 215 \text{ Mev},$$
$$\theta^{0} \rightarrow 2\pi^{0} + 225 \text{ Mev},$$ [8]

this would be considered strong evidence that at least the two-pion and three-pion decays resulted from the decay of the same particle.

In 1953, Dalitz analyzed the tau decay. At this time most taus had been found in single glass-backed films of emulsion; the glass-backed film technique generally did not permit identification of the charge of the pions; therefore Dalitz's 1953 analysis was an average over the pion charges.[9] Later, the technique of stacking emulsion films into solid blocks of emulsion became general,[10] and it was possible to identify the pion charge in more cases. Dalitz then presented his analysis for known pion charges. Fabri has restudied the analysis in order to confirm Dalitz's main assumption (viz., that the momentum dependence of the decay amplitude is the simplest of those compatible with a given tau spin and parity), and made necessary relativistic corrections.[11] The Fabri form of the Dalitz analysis is reviewed in the next few paragraphs.

If the orientations of the decay-plane normal and the rotation of the decay configuration about the decay-plane normal are neglected,

then only two independent variables are necessary to describe the decay configuration for taus decaying at rest. These are $\vec{r}$, which is proportional to the distance between like pions, and $\vec{r}'$, which is proportional to the distance between the unlike pion and the center of mass of the like pion system. The momenta $\vec{p}$ and $\vec{p}'$ are the conjugate momenta, and $\vec{\ell}$ and $\vec{\ell}'$ the corresponding angular momenta (ℓ is even by Bose-Einstein statistics).

The conservation of angular momentum requires that the spin of the tau be the vector sum of $\vec{\ell}$ and $\vec{\ell}'$, i.e., $\vec{J} = \vec{\ell} + \vec{\ell}'$. The conservation of parity requires that the parity of the tau be the product of the intrinsic parity of the three pions and their orbital parity, i.e.,

$$P_\tau = (-1)^3 (-1)^{\ell+\ell'} = (-1)^{\ell'+1} .$$

The decay probability of the τ meson is obtained from first-order time-dependent perturbation theory, where the initial state is a τ meson with parity P and spin J, and with projection j in a given direction. The final state is a linear combination of all three-pion states, which are characterized by ℓ and ℓ' and have the same P, J, j as the tau. The square of the matrix element is given by Fabri as

$$F_{J,P} = \sum_j \left| \sum_{\ell,\ell'} c_{\ell\ell'}(P)\, S^{\ell,\ell'}_{J,0,j} \left\{ (2\ell+1)(2\ell'+1)(\ell'-|j|)!/(\ell'+|j|)! \right\}^{1/2} P_{\ell'}^{|j|}(\cos\theta) \right|^2 , \quad (\mathrm{I}.1)$$

where $S^{\ell,\ell'}_{J,0,j}$ are the Clebsch-Gordan coefficients and $\cos\theta = \vec{p}\cdot\vec{p}'/|\vec{p}||\vec{p}'|$.[11]

The relative decay probabilities $c_{\ell\ell'}$ are derived under the following set of assumptions:

(a) The free-pion wave functions are approximated by the lowest-order term in the expansion about the origin, i.e., the spherical Bessel function of order ℓ, $j_\ell \simeq (pr)^\ell/(2\ell+1)!!$.

(b) The interaction radius is a tau Compton wave length.

(c) Final-state Coulomb and pion-pion interactions are neglected.

(d) The interaction is independent of ℓ and ℓ'.

Using these assumptions, Fabri gives

$$c_{\ell\ell'} = A_{J,P} \frac{a_{\ell+\ell'}}{(\ell+\ell'+4)!!} \frac{(\ell+1)!!}{(2\ell+1)!!} \frac{(\ell'+1)!!}{(2\ell'+1)!!} \left(\frac{p}{M}\right)^{\ell} \left(\frac{p'}{M}\right)^{\ell'} , \qquad (I.2)$$

where $a_{\ell+\ell'}$ has modulus less than 1 and decreases with $\ell+\ell'$; M is the tau mass. Both p and p' are much less than (M(c=1), so that under the above assumptions for a given initial state (J, P), only the $c_{\ell\ell'}$ with $\lambda = \ell+\ell'$ = minimum are important; in fact all other $c_{\ell\ell'}$ are less by at least two orders of magnitude.

The validity of these assumptions has been discussed by Dalitz,[9] Fabri,[11] and Eisenberg,[12] with the following conclusions. If the interaction radius were a pion Compton wave length, (a) would still be reasonable and the major effect would be to replace M by m(the pion mass) in $c_{\ell\ell'}$, perhaps necessitating the inclusion of terms of higher order in λ. Dalitz has proposed a method for treating separately the final-state Coulomb and pion-pion interactions. The Coulomb interaction is small ($\sim$1 Mev)and the pion-pion interaction[13,14,15] is unknown. Eisenberg states, however, that the only possible effect of such interactions would be to increase the interaction radius to a pion Compton wave length. Assumption (d) is the most critical, for if the interaction is strongly dependent on ℓ and ℓ' [13, 14, 15] the $c_{\ell\ell'}$ will differ grossly from those computed above. Furthermore, there may be partial or absolute selection rules for some values of ℓ and ℓ'. Even in the spirit of the Dalitz analysis, Assumption (d) may not be taken to exclude magnitude variations on the order of unity or phase difference of $a_{\ell+\ell'}$ in the degenerate cases (those for which there are more than one term with $\ell+\ell'$ = min).

Dalitz[16] and, later, Amaldi[17] compared the Dalitz theory with all τ's whose charge was known, and concluded: (a) for spin less than 4 and τ and θ do not have compatible spin and parity, and (b) a

pseudoscalar tau was quite possible. Conclusion (a) was based on the distribution in cos θ, which is thought to be insensitive to bias. Conclusion (b) depends critically on bias. The obvious biases are:

(1) a geometric bias, brought about because the finite dimensions of the emulsion stack in which it is necessary to bring at least two pions to rest restrict certain decay configurations;

(2) a bias brought about by area scanning (which may depend on grain count at minumum ionization as well as the decay configuration).

Brene et al.[18] have recently derived the effect of the geometric bias as a function of the number of emulsion plates in a stack. The scanning bias is very difficult to evaluate and consequently must be eliminated (e.g., by use of scanning technique that is independent of the decay configuration.) The samples used by Dalitz[16] and Amaldi,[17] composed primarily of cosmic-ray τ mesons for which the finding rate was low, represented efforts of many workers, and none of the contributions was corrected for the above bias.

Teucher et al. suggested an independent test for the spin of the tau, which consists in examining the orientation of τ decay planes for possible polarization effects.[19,20] In general, if the tau has a spin, a polarization effect would be expected (though not necessarily found)--especially near production threshold. There are reasons to believe that a beam of polarized taus would not be depolarized while being brought to rest unless the tau has a high anomalous magnetic moment.[21,22] Clearly, a null result would not indicate a spinless tau, whereas a positive effect would be a clear indication of a tau with a spin.

Even after inception of Bevatron operation little new knowledge about K mesons was gained until the development of the Kerth-Stork strong-focusing magnetic spectrometer.[23] This system made it possible to accurately measure the mass of K-meson modes by application of the range-momentum method,[3] and in conjunction with scanning by track-following, the K-meson finding rate was increased by several orders of magnitude. Subsequent experiments to measure

mass,[3,4,5] lifetime,[7] and excitation function,[4,5] indicated that these parameters are very nearly the same for the principal modes of decay of the K meson. These results, in the light of the Dalitz-Amaldi conclusion (that a tau could not decay into two pions) leaves us with at least two different particles, which happen to have almost the same mass, lifetime, and excitation function.

Several conjectures have been advanced to explain this apparent mass degeneracy.[24-27] Some authors would have the τ (or θ) have a significant branching ratio of gamma decay to θ (or τ) where the daughter lifetime is a great deal less than that of the parent.[24,25] Then the apparent masses as measured by range-momentum method would be the same, but the mass as measured by energy released in decay would be less for the daughter. Although the degeneracy may be accidental, the possibility that it may be a necessary degeneracy has been exploited. Lastly, the nonconservation of parity is a possible explanation.

In any event, it is important not only to re-examine the Dalitz-Amaldi conclusion, but to measure the masses of the K-meson modes by the range-momentum method and by measuring energy release in decay. A significant mass difference between the two mass measurements would critically affect the above conjectures. This thesis discusses one aspect of a systematic investigation of the K meson, as described above, by the members of the Richman group.

C. Experimental Method

The technique used in this emulsion experiment depends upon the production of the K^+ mesons at a laboratory angle of 90° and on the fact that their lifetime is long enough to traverse (without significant diminution) a magnetic analyzer and focusing system external to the Bevatron vacuum system. This K-meson beam is arrested in a known volume of three separate emulsion stacks large enough to stop most pions from the tau decay.

The track-following method of scanning for K mesons is employed. The ranges and direction cosines (relative to a Bevatron coordinate system) of the pions resulting from the tau decay are measured by use of high-power microscopes and calibrated stages. Measurement of the ranges yields the pion energies, the Q of the tau, and the decay configuration. Pion-direction cosines are used to test each decay for coplanarity and for momentum balance. The possible spin-parity assignments of the tau are obtained from the Dalitz analysis.

II. EXPERIMENTAL ARRANGEMENT

A. K Beam

The general experimental arrangement is shown in Fig. 1 and the essential elements of the strong-focusing spectrometer are shown in Fig. 2.

A target was plunged into the 6.2-Bev proton beam in one of the straight sections of the Bevatron. Particles of proper charge and momentum coming from the target at 90° to the incident beam passed through the 0.090-inch aluminum wall of the Bevatron vacuum tank, then through a compound lens formed by a series of quadrupole magnets, and were brought to a focus in a stack of nuclear emulsions placed behind a momentum-analyzing magnet. The flux of positively charged particles consisted mainly of protons, K mesons, and pions. The momentum selection of the analyzing magnet restricted the protons entering the stack to ranges typically in the vicinity of 1.5 cm and the K mesons to about 7 cm, while the pions passed completely through the stack. Brass was placed on the low-energy side of the magnet to shield the detector from neutral radiation from the target, and a considerable amount of lead and concrete was also used to shield from beam "spill-out" during the early part of the accelerating cycle and from associated secondary radiation. The copper target used was 3/8 inch high and 5/8 inch in the proton beam direction. The aperture of the lens was 2 inches and the analyzing magnet had a 2.5-inch gap.

In order to obtain sufficient strength in the lens it was necessary to use four quadrupole magnets. The first two formed a lens converging vertically and diverging horizontally, while the latter two magnets were operated so as to diverge vertically and converge horizontally. The compound lens formed by these two elements was both vertically and horizontally convergent; however, it was astigmatic. Since the momentum resolution of the system was determined largely by the horizontal size of the target image at the stack there was an incentive to minimize the horizontal magnification to a value that was satisfactory in consideration of the concomitant increase in the vertical magnification. If the

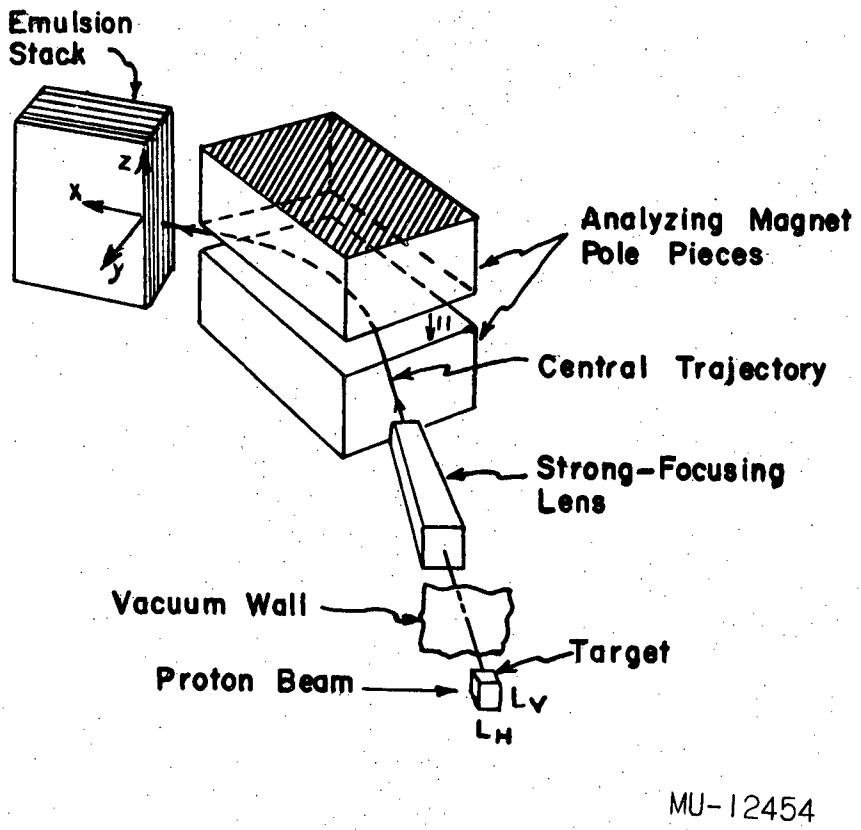

Fig. 1. Sketch of the basic experimental arrangement, indicating the Bevatron coordinate system to which the direction cosines of the pions are referred.

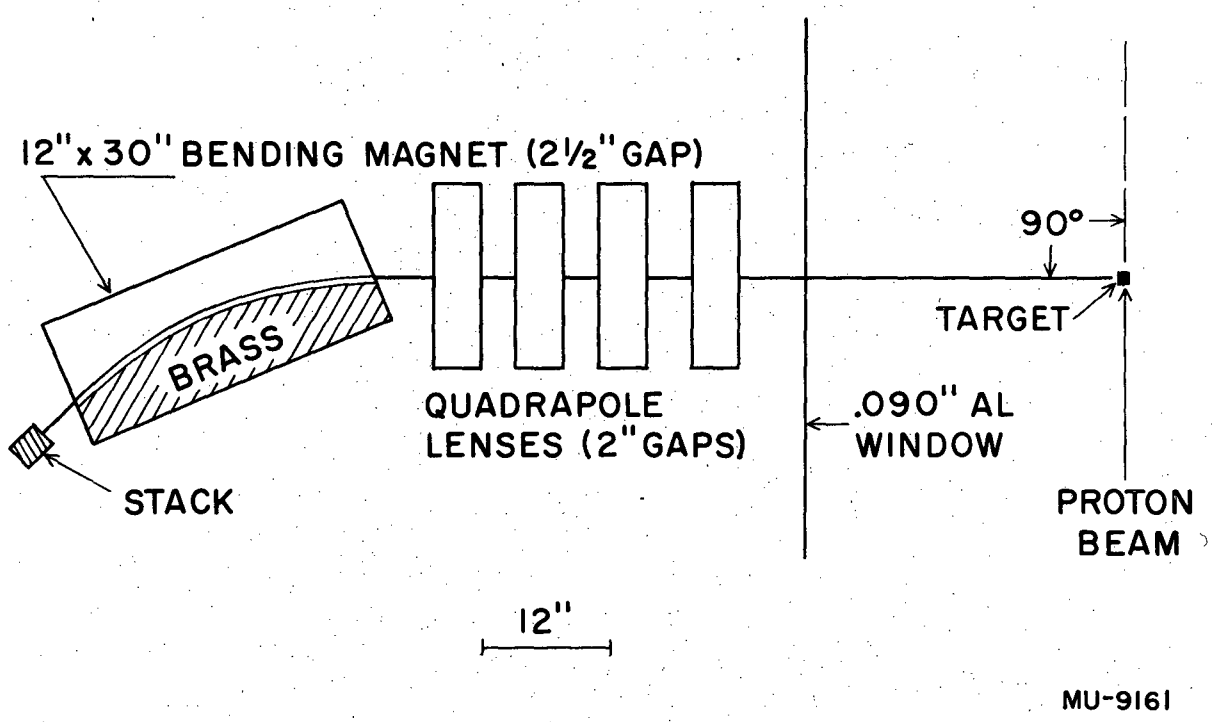

Fig. 2. The strong-focusing spectrometer.

latter became too large, particles would be lost by striking the pole pieces of the analyzing magnet. The horizontal magnification used was about 0.6 x, and the vertical magnification was about 1.5 x.

Proper current values for all the magnets were obtained from a series of wire-trajectory measurements made for particles of momenta in the vicinity of 360 Mev/c. This method was found to be quite satisfactory in achieving proper focus and magnification conditions. The measurements were made considerably easier and more accurate by a current regulator, constructed by Mr. Leroy Kerth, which compensated for currents indiced in the wire by motion in the magnetic field.

The trajectories obtained from these wire measurements were used to position the stacks when the exposure was made, so that the particles would enter approximately perpendicular to the front face of the stacks.

The exposures were monitored by (a) a counter telescope, located above the Bevatron tank, that measured secondary-particle flux from the target; (b) a series of test exposures measuring the proton flux of the stack, using 1-by-3-inch glass-mounted 50-μ G.5 emulsions, which were exposed, developed, and scanned during the exposure, and (c) the Bevatron permanently installed proton-beam monitor ("induction electrodes"). The total proton flux required at the stacks was estimated from the previously obtained ratio of K mesons to protons, and was measured by correlating the sampled data from Method (b) with the relative primary-proton beam flux obtained from (a) and (c).

B. Stacks

Three large stacks of 600-μ Ilford G.5 electron-sensitive emulsion were used. Designation and particulars of each stack are presented in Table I. The stacks were made by firmly clamping the emulsion sheets together (without tissue paper between the pellicles) between two sheets of bakelite. All four stack edges were machined to close tolerances to permit accurate measurements of the volume of the stack and thus of its density. Fiducial marks for aligning the emulsions after development were provided at various points by exposing the milled sides to x-rays passed through a slit system. Tabs placed on the glass-mounted, developed emulsion were ground until the x-ray marks on neighboring plates were aligned.

Table I

K-Particle Exposure Energy and Stack Parameters for each Stack

Stack number	K-beam energy (Mev)	Number of Pellicles	Pellicle area (in.)	Average pellicle thickness (microns)	Stack density (g/cm^3)
16	114	107	3.5 x 3.5	599	3.785
17	170	40	3 x 6	620	3.880
20	114	95	9 x 17.5	594	3.800

III. MICROSCOPE WORK

A. Scanning by Track-Following

K mesons entered the stacks with a relative ionization about 1.8 times minumum. A swath perpendicular to the general beam direction and about 1 cm behind the stopping protons was scanned for tracks whose grain densities were from 1.5 to 3.0 times minimum (pions were at minimum). Such tracks were followed, and if they stopped in about 4 cm and multiple-scattered appropriately, they were identified as K mesons. Endings were examined to determine the decay mode. This method of scanning is thus unbiased with respect to the tau-decay configuration.

B. Measurement of Pion Ranges

1. Method

Two different criteria were used to measure the pion ranges, depending on whether or not the ranges were used in the Q measurement. For those used in the Q measurement the average plate thickness (Table I) was used to compute the chord between points where there was either an integrated 10° change of pion direction, or a visible change in the diving rate. For those ranges not used in the Q measurement, a similar precedure was followed, using a 20° criterion. The range of the pion was taken to be the sum of these chords (corrected for air gaps between pellicles).

2. Errors

a. Air Gaps. The average densities of the emulsion stacks, obtained from their measured areal densities (σ = mass per unit area) and the thickness of the stacks, were 0.7% to 1.1% less than 3.826 g/cm^3, which is the density for Ilford G.5 emulsion when it is shipped from the factory. From measurements of individual pellicles of fresh emulsion it is evident that there is little water loss through the shipping wrappings.

There also should be little change in the density in the process of stacking the emulsion or by evaporation or absorption through the edges of the machined stack. The difference between the average density of the stacked emulsion and of individual pellicles is attributed to air gaps between pellicles. The air gaps (about 5 microns on the average) increase the total stack thickness above its true value and so reduce the stack density.

Let t_m and ρ_m be the measured average plate thickness and density for the stack, and t_t and ρ_t the true average thickness and density of the emulsion. The ranges of the pions can then be computed as follows:

(a) The value t_m is used to obtain the shrinkage factor. This gives the length of the track through both emulsion and air.

(b) The true density ρ_t is assumed to be 3.826 g/cm^3.

(c) The average air gap thickness, t_a, is taken to be

$$t_a = t_m - t_t = \sigma\,(1/\rho_m - 1/\rho_t).$$

(d) The range in emulsion alone, R_E, is then obtained from

$$R_{E_i}/R_i = Z_{E_i}/Z_i = Z_i - N_{a_i}\ t_a/Z_i\ ,$$

where R_{E_i} is the length of the ith chord in emulsion,

R_i is the length of the ith chord in emulsion and air,

Z_{E_i} is the vertical height between chord ends in emulsion,

Z_i is the corresponding height through air and emulsion,

N_{a_i} is the number of air gaps traversed.

Then we have

$$R_E = \sum_i R_{E_i}$$

b. Range straggling and reading error. These determinate errors, which are statistical in nature, are not explicitly computed. They affect the spread of the Q distribution but not its average value. In the following sections errors are considered which may be systematic.

c. Alignment. Generally the position of neighboring plates is known to within 25 microns, from the x-ray fiducial marks, but there was some systematic shifting of the stacks. To eliminate or reduce this shifting the coordinates of the x-ray marks were measured on a microscope stage and used as corrections.

d. Stage-stop error. This error arises when the tabs have not been properly positioned against the microscope stage stops. The effect is to introduce an error which is the same regardless of the number of plates between chord and points. It is estimated to be 25 to 50 microns, which is negligible for the average pion (range about 1 cm); for short tracks that pass through one or more plates however, it may be significant.

e. Distortion and Rub-off Errors. The distortion and rub-off errors enter to first approximation as errors in the position of both tau and pion decay. An error in the position of an intermediate point such as to increase any one chord length reduces the following chord length. These errors are then negligible.

f. Range Shortening. The percent difference between the arc and chord lengths along a pion track was estimated to be 0.48% in range for ranges measured by the 10° criterion. This estimate is good to 30%. The uncertainty of 30% is due mostly to an uncertainty in how closely the 10° criterion was followed.

C. Measurement of Direction Cosines

1. Method

The direction cosines of the pions were measured by a microscope equipped with a goniometer and a calibrated reticle. Thus the angle of a track θ_i, the length of a track in the plane of the emulsion ρ_i, and the rise of a track ΔZ_i were measured. These measurements relative to the microscope system are then transformed to the Bevatron system (Fig. 1).

2. Errors

The microscope field of view, although not all in focus (i.e., flat), fell off symmetrically from the center. Therefore the center of the pion track to be measured was placed in the center of the field of view so that the ends were essentially on the same isofocus contour. The end points of the measured track section were distinct grains in the track. This greatly improves the measurement of ρ and especially ΔZ. The length of track was in general not over 100 microns, and in most cases about 50 microns, since the longer the track the more likely a large scatter in Z. In fact, on some of the first measurements on tracks 200 microns or so in length, the cases which at first appeared to be noncoplaner were shown to be scattering out of the plane of the emulsion (i.e., this was a scatter in Z).

The effect of measurement errors and multiple scattering is derived in Appendix A by the usual method of propagating errors. The direction cosine errors are used to estimate the expected errors in momentum balance and coplanarity. Since an estimate is all that is desired, it is convenient to arrive at an average set of measurement errors to facilitate the calculations. Some of the considerations used in arriving at a suitable set of measurement errors are as follows.

a. Error in angle (S_θ). For reasonably flat tracks ($< 45^\circ$) and high-energy pions (>20 Mev), the error in measuring angles is insignificant, i.e., about 0.2°. Furthermore, multiple scattering in the plane of the emulsion can be greatly reduced because such tracks are not "clogged" and a best fit to the tracks with the reticle is easily obtained. For steep tracks, low-energy pions, or both, the uncertainty in angle can be of the order of 2.0°. It was felt that 0.37° represented a suitable average error.

b. Error in $\rho(S_\rho)$. The primary measurement is the length of the track projection in reticle units (r); this must be multiplied by a conversion factor (f) to obtain ρ in microns. The conversion factor f was measured to 1% with the microscope stage; an error of 2/3 reticle units is a pessimistic estimate of the reading error. The latter takes into account the scatter of a grain about its true position.

c. Error in $z(s_z)$. The rise of the measured track section, z', (measured with the Z screw of the microscope) is multiplied by the shrinkage factor (s) to obtain z, (the rise before development.) The shrinkage factor is the ratio of the plate thickness before development (t_b) to the plate thickness after development (t_a), and the error in s due to the errors in t_a and t_b is about 1.8%. The reading error is taken to be 0.6 microns, which includes the scatter of the grain about its true position.

d. Effect of multiple scattering on the direction cosine. Multiple scattering in the plane of the emulsion is greatly reduced because the projected track section is judged to be straight by comparison with a cross hair in the microscope reticle eye piece. This sets an upper limit on ρ. The effect of multiple scattering out of the plane of the emulsion (multiple scattering in Z) is considered in Appendix A-1. The projected rms scattering angle is used, and we note that one should

instead use the projected rms scattering angle, subject to the condition that the scattering appear to be small in the orthogonal plane.

e. Effect of direction-cosine errors on coplanarity. The angle δ is that included between the normal to the plane containing two of the pions and the third pion. The effect of the direction-cosine errors on $\cos\delta$ is computed in Appendix A-2. Figure 3 shows a histogram of number vs normalized deviation--i.e., $\cos\delta/S\cos\delta$--and also shows (for reference) a gaussian with unit standard deviation. Because we have chosen a single set of measurement errors, which is large for most cases and small for a few cases, we should expect this to make the good cases better and the bad cases worse. This is demonstrated in Fig. 3, where the histogram has a standard deviation of 0.84. We conclude that these taus are coplanar within measurement errors.

In a few cases the tau decayed at the surface of an emulsion sheet, hence one or more pions were not visible at the tau decay. For these cases the angles between pions could not be accurately estimated, and momentum balance and coplanarity were not computed.

f. Effect of direction-cosine errors on momentum balance. Components of the momentum unbalance along the x, y, and z directions are ΔP_x, ΔP_y, and ΔP_z respectively, and total momentum unbalance is $\Delta P = \sqrt{\Delta P_x^2 + \Delta P_y^2 + \Delta P_z^2}$. The effect of the direction-cosine and energy errors on the momentum balance is computed in Appendix A-3. The estimate of the energy error was obtained from the Q distribution (discussed next). Figures 4 and 5 show histograms of number vs normalized deviation for ΔP_x and ΔP respectively. These figures also include reference curves obtained by assuming that ΔP_x, ΔP_y, and ΔP_z are independent and normally distributed with unit standard deviation. As for coplanarity, the result of choosing an averaged set of measurement errors is to decrease the standard deviation of the histograms. We conclude that, for these taus, momentum is balanced within measurement and energy errors.

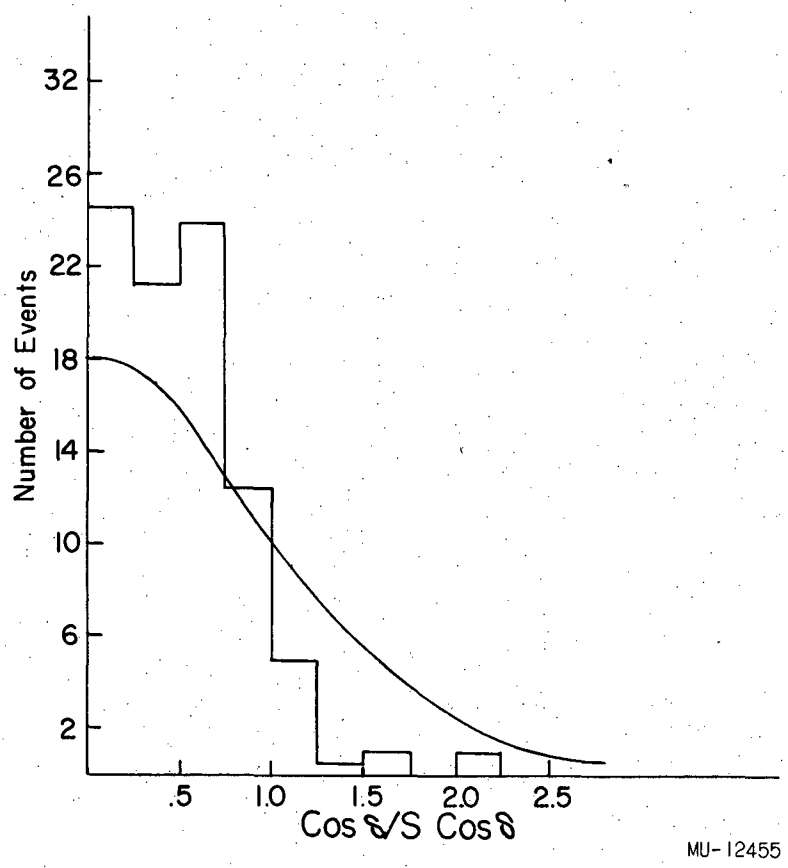

Fig. 3. This histogram shows the deviation from coplanarity when an attempt to estimate the measurement errors and take into account multiple scattering has been made. The angle δ is included between the normal to two of the pions and the third pion which will be 90° for a coplanar tau.

The quantity S cos δ includes estimates of the measurement errors and effect of multiple scattering. The curve included in the plot is a gaussian with unit standard deviation. It is presented for reference because the true distribution is expected to be symmetric about the origin and nearly Gaussian.

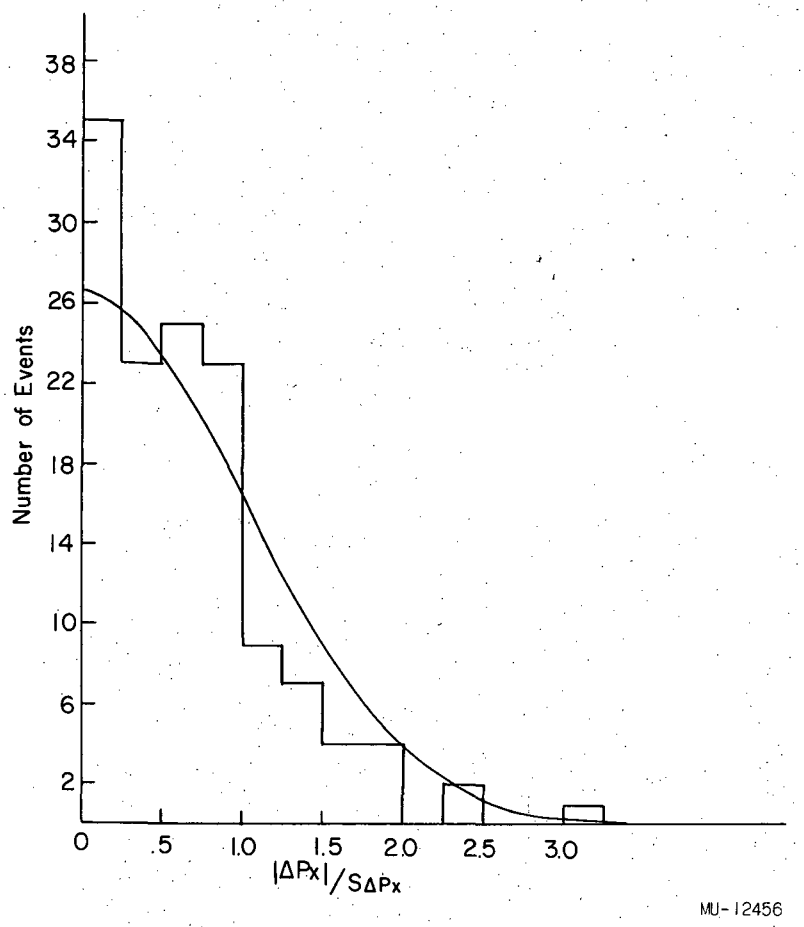

Fig. 4. Plot of the momentum unbalance distribution along a coordinate axis normalized by an estimate of error which includes measurement errors, energy errors, and the effect of multiple scattering. A gaussian with unit standard deviation is also shown for reference.

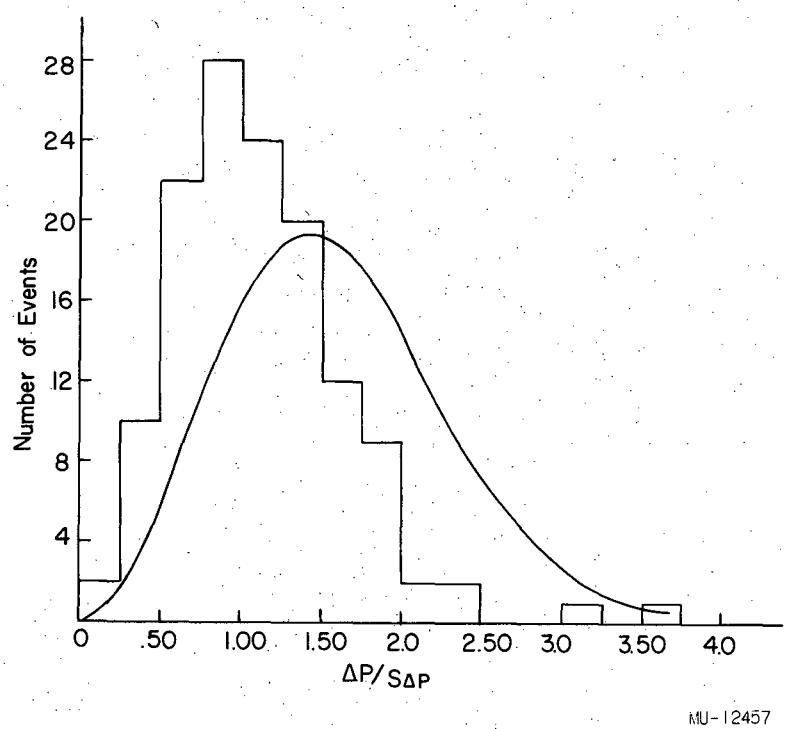

Fig. 5. A histogram showing the total momentum unbalance normalized by an estimated error which includes measurement errors, energy errors, and the effect of multiple scattering. The curve shown for reference was derived by assuming that the momentum unbalance along each coordinate axis was independent and normally distributed.

IV PION ENERGY AND MASS OF TAU MESON

A. Method

The mass of the tau is obtained by measuring the energy release Q of the tau decay in conjunction with the known pion mass.[28] The sum of the pion energies yields the Q in which the pion energies are obtained by measuring the pion ranges and using the range-energy relation given by Barkas ans Young.[29] When only two pions stay in the stacks the energy of the other pion is obtained from the energies and the angle between the stopped pions (the conservation of momentum is assumed).

B. Discussion of Q

To obtain the average Q of the tau, a sample of 67 taus was chosen. For these taus, all three pions stopped in the stack and none of the pions made a large-angle scatter. The pion ranges were measured by the 10° criterion discussed in Section III-B. We recapitulate the conclusions of this section. An investigation of possible sources of systematic error showed that the resulting errors, with the exception of range shortening, either were small or tended to be randomly distributed. Because randomly distributed errors only increase the spread of the Q distribution, their effect is included in its standard deviation. The range-shortening error was estimated to be 0.25% in energy. These ranges were corrected for air gaps (the emulsion was assumed to have a density of 3.826 g/cm^3). Any uncertainty in this density (ρ_t) is due to an uncertainty in the equilibrium value of the relative humidity of the emulsion. Because the stopped power of emulsion per g/cm^2 is a slowly varying function of its water content (relative humidity), an error in the ρ_t leads to a relatively smaller error in Q. The effect of an error in ρ_t on the Q values is given (see Appendix B) by

$$\Delta Q/Q = -0.046\, \Delta\rho/\rho\,. \qquad \text{(IV-1)}$$

Barkas and Young[29] give the density of emulsion at 35% relative humidity as 3.90 g/cm^3. This is the upper limit of the emulsion density, and the measured stack density is the lower limit. Inspection of Eq. (IV-1) shows that for 1% error in the emulsion density the error in the average Q is 0.05%, or $\Delta Q = 0.04$ Mev. The error in Q due to the uncertainty in emulsion density is therefore negligible.

The range-energy relation given by Barkas and Young[29] was used. It is based on Vigneron's parameters; in particular, the mean ionization potential of 322 ev is used to extrapolate to high velocity. This relation is for Ilford C.2 emulsion of density 3.815 g/cm^3 at a relative humidity of 55% Ilford G.5 emulsion has the same composition, however. The discrepancy in densities between them (i.e., G.5 has a density of 3.826 and C.2 a density of 3.815 at 55%) is not considered. Stack 17 had a density greater than 3.826 (see Table I) and a new range-energy relation was made, using the method suggested by Barkas and Young[29] and the range-energy relation in water from Rich and Madey.[30]

C. Results

An average Q of

$$
\begin{aligned}
74.94 &+ .19 \text{ Mev (range shortening)} \\
&\left.\begin{matrix} +.04 \\ -.07 \end{matrix}\right\} \text{ Mev (uncertainty in water content of emulsion)} \\
&\pm .18 \text{ Mev (standard deviation of the average } Q) \\
&\pm .17 \text{ Mev (error in measurement of the stack density),}
\end{aligned}
$$

or $75.13 \pm .20$ Mev,

was obtained. Figure 6 shows the distribution of Q values. This distribution is quite consistent with a normal distribution (which is also plotted).

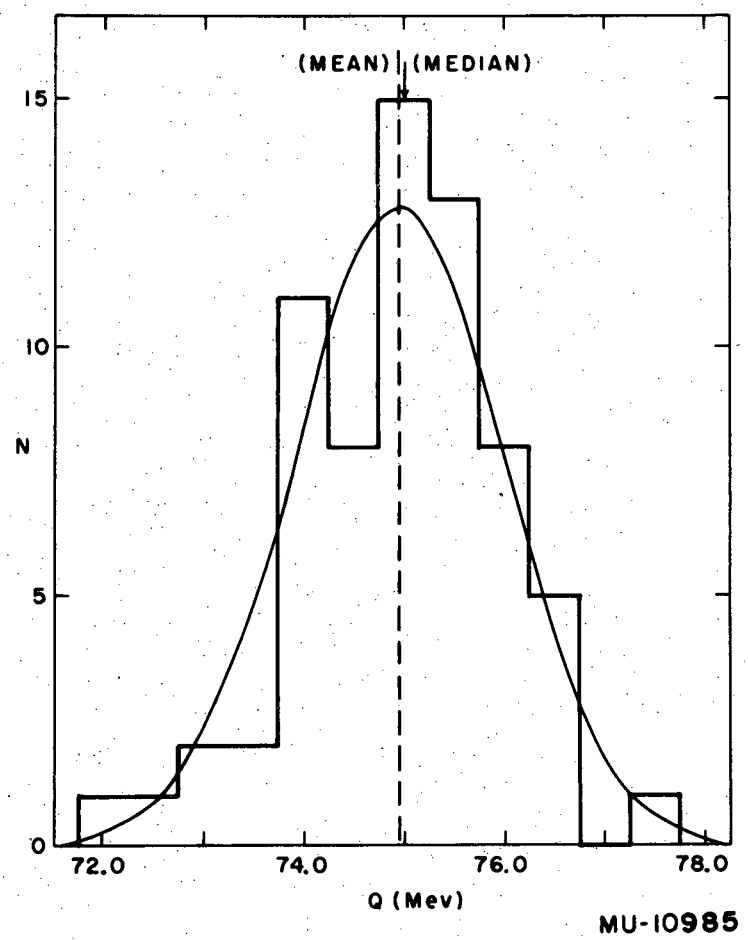

Fig. 6. Plot of the distribution of Q values for 67 taus which had all three pions staying in the stack and none of the pions making a large-angle scatter. The average Q is 74.94 Mev and the median is 75.0 Mev. The distribution is fitted with a normal curve and the agreement is observed to be quite good.

The corresponding mass of the tau (in electron mass, m_e) is

$$
\begin{aligned}
966.1 &+ .37\ m_e \text{ (range shortening)} \\
&\left.\begin{matrix} +.08\ m_e \\ -.14 \end{matrix}\right\} \text{(uncertainty in water content of emulsion)} \\
&\pm .36\ m_e \text{ (standard deviation of the average Q)} \\
&\pm .44\ m_e \text{ (error in measurement of the stack density)} \\
&\pm .62\ m_e \text{ (standard deviation of the pion masses),}
\end{aligned}
$$

or $966.5 \pm .74\ m_e$.

The pion masses from Barkas, Birnbaum, and Smith[28] were used. These are

$$m_{\pi^+} = 273.3 \pm 0.3\ m_e ,$$
$$m_{\pi^-} = 272.8 \pm 0.4\ m_e ,$$

where the errors indicated are standard deviations.

V. SPIN AND PARITY

A. Design of Experiment

1. Selection of a Bias-free Sample

This experiment was specifically designed to avoid any bias due to scanning technique or of a geometric nature (see Sec. I-B). The geometric bias was almost totally eliminated by chossing the stack dimensions about twice the maximum range of a pion resulting from the tau decay. (Stack No. 16, the first exposure made by the Richman Group in the Kerth-Stork beam, was a 3.5-inch cube, as suggested by Robert W. Birge for exactly this reason). The degree to which geometric bias was reduced is illustrated by the fact that of 192 taus only two had a single pion stopped in the stacks. Scanning bias was eliminated because only taus found by systematic track-following are included in this analysis. This includes 179 out of a total of 192 taus found. Omitting the two taus with only one pion stopped, the sample we discuss has a total of 177 taus.

2. Coplanarity and Momentum Balance

The Dalitz analysis is valid only if the sum of the pion momenta is zero ($\vec{P}_1 + \vec{P}_2 + \vec{P}_3 = 0$). To insure that the sample complied with this requirement, both coplanarity and momentum balance were checked. A coplanarity test (Sec. III-C-2e) tells only about errors out of the decay plane, while momentum balance is three-dimensional (Section III-C-2f). However, for taus with only two pions stopped in the stack, or if one of the pions makes an inelastic scatter, momentum balance is used to obtain the energy of the third pion so that in these cases only a coplanarity test can be used. As stated previously in Section III-C-2e and III-C-2f the taus discussed in this analysis balanced momentum and (or) were coplanar within measurement errors.

3. Statistics and Sample Size

It was decided that a χ^2 test would be used to discriminate between various cases of spin-parity. The procedure is to test the

theoretical distribution for each case of spin-parity against the experimental distribution and to find the probability that the latter distribution would result from random fluctuations from the theoretical distribution. This probability is called the Pearson probability. It is an accurate estimate, provided at least five intervals with at least 10 events in each interval are used. To comply with these requirements the energy spectrum and angular distribution are each divided into five intervals such that about 10 events are expected in each interval. Because these distributions are independent, we add the χ^2 obtained from each, and the Pearson probabilities are calculated for the sum of the degrees of freedom. A Pearson probability of 1% was used as a confidence level; i.e., if the Pearson probability for a case of spin-parity was less than 1% we rejected that case.

Differentiation between the various cases of spin-parity depends on the sample size and, to some extent, on which comparison test is used. Because we used a χ^2 test it was necessary to decide on the basis of it what the minimum number of taus must be for significant results. Such a decision is made when using a χ^2 test by the power test.[31] The power is the probability that a hypothesis will be rejected in favor of another when in fact the hypothesis is false, or--to put it another way--the power tells how "lucky" one may expect to be in attempting to distinguish between two hypotheses. A power of 1.0 means that a definite decision may be expected, and a power of 0.0 means no decision is possible. The power depends only on the theoretical hypotheses, the sample size, and of course, the confidence level. Table II gives the power for distinguishing the case of spin 0-odd parity [0 -] from all other cases that we shall consider, for samples sizes of 100 and 200. For the degenerate cases the minimum power is given.

Table II

Table of powers for sample sizes of 100 and 200 taus. Powers are presented in the form $1 - 10^{-X}$.

Spin-parity	Power: Sample size 100	Power: Sample size 200
Unique Cases		
1+	$1 - 10^{-2.74}$	$1 - 10^{-7.0}$
1-	$1 - 10^{-10}$	—
2+	$1 - 10^{-6}$	—
3-	$1 - 10^{-1.74}$	$1 - 10^{-5.60}$
Degenerate Cases		
2-	$1 - 10^{-0.08}$	$1 - 10^{-0.26}$
3+	$1 - 10^{-0.06}$	$1 - 10^{-0.08}$
4+	$1 - 10^{-1.2}$	$1 - 10^{-3.8}$
5-	$1 - 10^{-1.3}$	$1 - 10^{-4.2}$

We see that for samples sizes of between 100 and 200 taus we can expect to distinguish between $[0^-]$ and $[1+]$, $[1^-]$, $[2+]$, $[3^-]$; for samples of about 200 taus we can expect to distinguish between $[0^-]$ and $[4+]$ and $[5^-]$. We cannot expect to be able to distinguish between $[0^-]$ and $[2^-]$ and $[3+]$.

B. Discussion

To facilitate discussion of the details of Dalitz's analysis we recapitulates: The square of the matrix element is

$$F_{J,P}(p', \theta) = \sum_j \left| \sum_{\ell,\ell'} c_{\ell\ell'}(p') S_{JOj}^{\ell\ell'} \left\{ (2\ell+1)(2\ell'+1) \frac{(\ell'-|j|)!}{(\ell'+|j|)!} \right\}^{1/2} P_{\ell'}^{|j|}(\cos\theta) \right|^2$$

where $S_{JOj}^{\ell\ell'}$ are the Clebsch-Gordan coefficients. The relative decay probabilities ($c_{\ell\ell'}$) are derived under two essential assumptions: (a) that the interaction radius is a tau Compton wave length and (b) that final-state interactions can be neglected. Then we have

$$c_{\ell\ell'} = A_{JP} \frac{a_{\ell+\ell'}}{(\ell+\ell'+4)!!} \left(\frac{m}{M}\right)^{\ell+\ell'} \frac{(\ell+\ell)!!}{(2\ell+1)!!} \frac{(\ell'+1)!!}{(2\ell'+1)!!} \left(\frac{p}{m}\right)^{\ell} \left(\frac{p'}{m}\right)^{\ell'}, \quad \text{(V-2)}$$

where m is the pion mass and M is the tau mass. Both p and p' are less than m(c = 1), so that for a given initial state (J, P) only the $c_{\ell\ell'}$ with $\lambda = \ell+\ell'$ = min are important; in fact all other $c_{\ell\ell'}$ are less by at least two orders of magnitude. This reduces the computation of $F_{JP}(p', \theta)$ to only the pairs of ℓ, ℓ' to the left of the dotted line in Table III.

Table III

Pairs (ℓ, ℓ') for a τ with Spin J and Parity P

J	P	(ℓ, ℓ')	
0	+	-	-
	-	(0, 0)	(2, 2); (4, 4); ------
1	+	(0, 1)	(2, 1); (4, 3); ------
	-	(2, 2)	(4, 4); (6, 6) ------
2	+	(2, 1)	(2, 3); (4, 4) ------
	-	(0, 2); (2, 0)	(2, 4); (4, 2); ------
3	+	(0, 3); (2, 1)	(2, 3); (4, 1); ------
	-	(2, 2)	(2, 4); (4, 2); ------
4	+	(2, 3); (4, 1)	(2, 5); (4, 3) ------
	-	(0, 4); (2, 2); (4, 0)	(2, 4); (4, 2) ------
5	+	(4, 1); (2, 3); (0, 5)	(6, 1); (4, 3); (5, 2); ----
	-	(4, 2); (2, 4)	(6, 2); (4, 4); (2, 6); -----

There are five cases with an unique pair (ℓ, ℓ') with $\ell + \ell'$ = min.: (0 -), (1 +), (1 -), (2 +) and (3 -). There are four cases with only two pairs with $\ell + \ell'$ = min.: (2 -), (3 +), (4 +), and (5 -). We consider only these nine cases because with any more than two pairs there are enough free variables that a good fit is insured. Of these nine cases, five are compatible with the decay of the tau into two pions: these are: (1 -), (2 +) (3 -), (4 +), and (5 -). Table IV gives the square of the matrix elements, F_{JP}, for the cases to be considered.

Table IV

Square of Matrix Element

J P	F_{JP}
0 -	1
1 +	p'^2
1 -	$p^4 p'^4 \sin^2\theta \cos^2\theta$
2 +	$p^4 p'^2 \sin^2\theta$
2 -	$p'^4 + p^4 + 2\cos\phi\, p^2 p'^2 (3\cos\theta - 1)$
3 +	$p^4 p'^4 \sin^2\theta (5 + 3\cos^2\theta)$
3 -	$p'^6 + 21/16\, p^4 p'^2 (2+\cos^2\theta) + 3\sqrt{7}/4 \cos\phi\, p'^4 p^2 (3\cos^2\theta - 1)$
4 +	$p^4 p'^6 \sin^2\theta (1+\cos^2\theta) + (5/6)^3 p^8 p'^2 \sin^2\theta + (5/6)^2\sqrt{3/5}\cos\phi\, p^6 p'^4 \sin^2\theta(5\cos^2\theta - 1)$
5 -	$(p^4 p'^8 + p^8 p'^4)\sin^2\theta(1+9/7\cos^2\theta) - \cos\phi\, p^6 p'^6 \sin^2\theta(1 - 32/7\cos^2\theta - \cos^4\theta)$

For the degenerate cases, the ratio of a's was assumed to have unit magnitude but allowed for a phase difference of ϕ. In Appendix C the effect of increasing the interaction radius is considered and shown to be negligible in most cases unless the radius is several pion Compton wave lengths. Therefore, only the matrix elements of Table V are considered. These matrix elements are relativistically correct provided the relativistic relation between momentum and energy is used throughout. Although the tau Q is only 75.0 Mev, relativistic effects are as

large as 20% in some cases. A strictly relativistic treatment of the data and of the analysis was made.

The theoretical energy spectra and angular distribution are obtained from $F_{JP}\rho \, dT d \cos\theta$, where ρ is the phase space. The following formulae were found useful in deriving these distributions:

$$\cos\theta = P_1^2 - P_2^2 / [2P_3^2(P_1^2 + P_2^2 - P_3^2/2)]^{1/2}, \qquad \text{(V-3)}$$

where $P_i^2 = T_i(T_i + 2m)$, T_1 and T_2 are the kinetic energy of the like pions ($T_1 > T_2$), and T_3 is the energy of the odd pion;

$$p'^2 = 3/2\, T_3(T_3 + 2m),$$

$$p^2 = M(T_M - T_3)[1 - 2/3\, p'^2 \cos^2\theta/(M - m - T_3)^2]^{-1}, \qquad \text{(V-4)}$$

where $T_M = (M + m)\, Q/2M$ is the maximum kinetic energy of a pion from a tau decaying with energy release Q;

$$\rho \propto \frac{(T_3 + m)p' p^3[(M - m - T_3)^4 - 4/3\, p^2 p'^2 \cos^2\theta]}{(T_M - T_3)(M - m - T_3)^2}$$

Computation of all the very tedious integrals involved in the calculation of the distributions was done by the IBM-650 Computing Machine. Figures 7 and 8 show the angular distribution for the unique and degenerate cases, respectively, and Figs. 9 and 10 show the energy spectra for the corresponding cases. For the degenerate cases the best fit to the experimental distribution are shown. In Appendix D the parameters for each tau are listed.

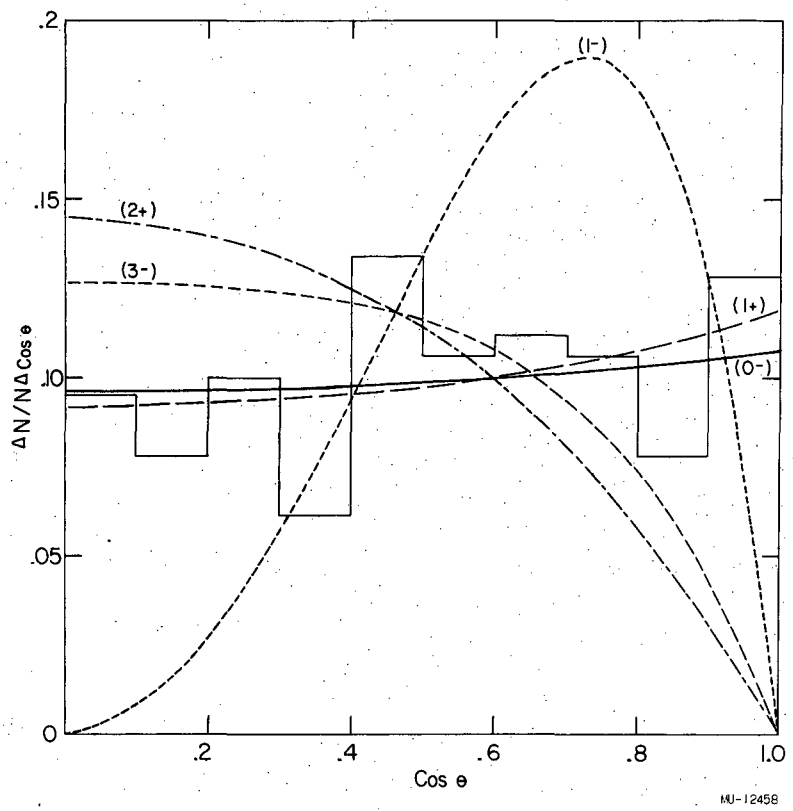

Fig. 7. This figure shows the expected angular distribution and the experimental histogram for the unique cases of the tau spin-parity; (0 -), (1 +), (1 -), (2 +), and (3 -). The curves shown are plotted by connecting the expected number in each interval. The angle θ is included between the relative momentum of the like pions and the momentum of the unlike pion. The cases of (0 -) and (1 +) give a very nice fit.

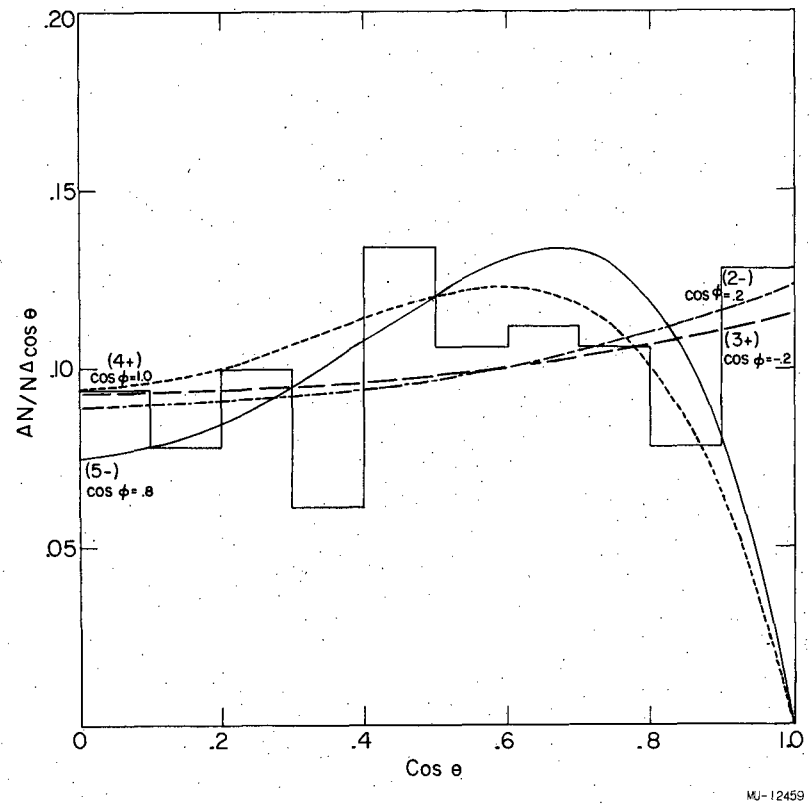

Fig. 8. Plot of the expected angular distribution and the experimental histogram for the degenerate cases of the tau spin-parity: (2 -), (3 +), (4 +), and (5 -). The curves shown are plotted by connecting the expected number in each interval. These curves were adjusted by varying the phase angle, ϕ, until a best fit was obtained (the value of the cos ϕ which the curve corresponds to is indicated). The angle θ is included between the relative momentum of the like pions and the momentum of the unlike pion. The cases of (2 -) and (3 +) give a good fit and also are very close to the cases of (0 -) and (1 +) shown in Fig. 7.

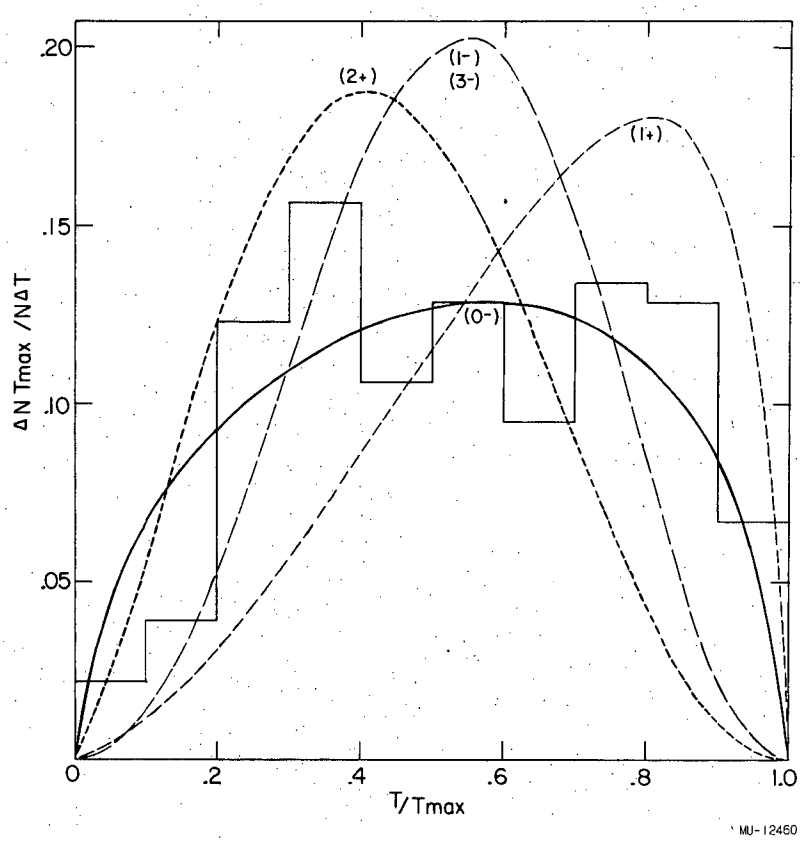

Fig. 9. This plot shows the expected energy spectra and experimental histogram for the unique cases of spin-parity. The theoretical curves are plotted by drawing a smooth curve through the expected number in each interval. The variable is the odd pion energy divided by its maximum possible value. The case of (0 -) is observed to agree well with the experimental distributions.

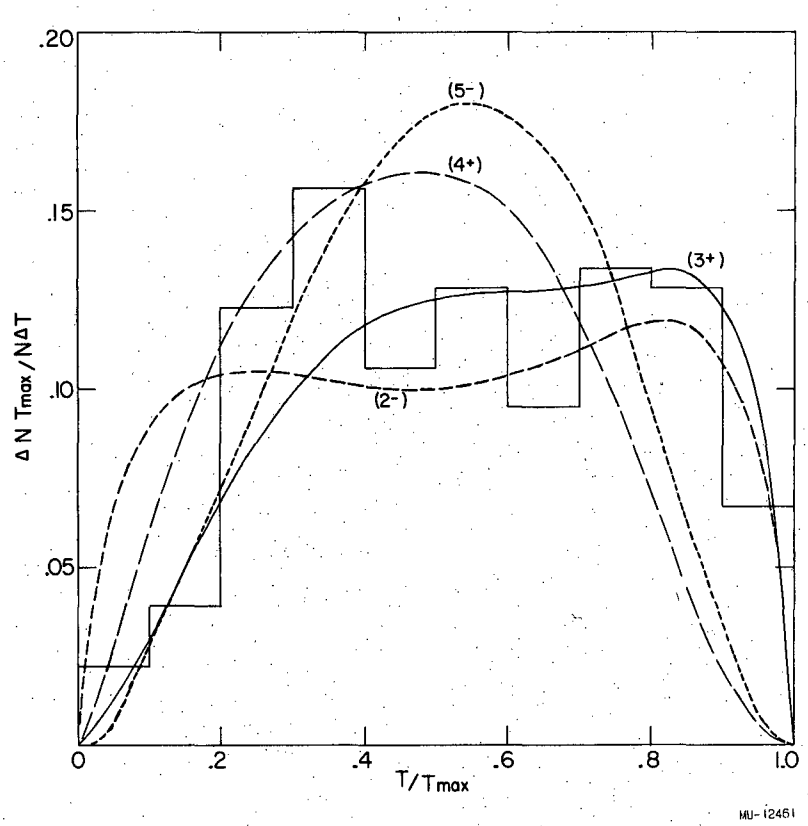

Fig. 10. This plot shows the expected energy spectra and experimental histogram for the degenerate cases of spin-parity. The theoretical curves are plotted by drawing a smooth curve through the expected number in each interval. The energy spectra are very insensitive to the phase between degenerate states and in fact in the classical cases are independent of it. The variable is the odd pion energy divided by its maximum possible value.

C. Results

Table VI lists the Pearson probabilities for each spin-parity case. These were obtained by the procedure described in Section V-A-3. For the degenerate cases the maximum probability is given.

Table V

Pearson Probability		
	J, P	Probability
Unique Cases		
	0-	$10^{-0.4}$
	1+	$10^{-11.3}$
	1-	10^{-30}
	2+	10^{-30}
	3-	$10^{-23.1}$
Degenerate Cases		
	2-	$10^{-0.38}$
	3+	$10^{-0.13}$
	4+	$10^{-16.0}$
	5-	$10^{-8.1}$

The result is that (0 -), (2 -), and (3 +) are all equally likely, whereas all other cases are either highly unlikely or have a probability, that for all practical purposes is nil. Further, none of the likely cases has spin-parity compatible with decay into two pions.

VI. POLARIZATION

A. Method

Information concerning possible polarization effects is obtained by inspecting the distribution of tau decay-plane normals and the distribution of odd-pion directions. A convenient set of variables to describe these distributions are the Eulerian angles Θ, Φ, and Ψ. We have taken the Eulerian angles that defined as follows: rotate by Φ about the z axis in a counter-clockwise direction from the x axis (this defines the line of modes), then rotate about the line of modes by an angle Θ (this defines a new polar axis, z'), and then rotate about z' in a counter-clockwise direction by an angle Ψ from the line of modes. The x, y, z are the coordinate system of Fig. 1 and z' is along the odd-pion direction. Here Θ and Φ define the decay-plane normal and Ψ defines the position of the odd pion in the decay plane.

B. Discussion and Results

A sample was taken which included all the taus in stacks No. 16 and No. 20 that were found by systematic track-following. These taus have a nominal energy of 114 Mev. Although they passed through the Bevatron's magnetic field and the strong-focusing spectrometer, the only possible effect of these fields is to rotate the direction of polarization of the tau beam. They enter the stacks and are arrested in about 7 cm. The effect of slowing down on a polarized proton beam has been investigated,[22] down to energies at which polarization disappears for other reasons, and was shown to maintain its polarization. Nothing is known experimentally about the depolarizing effects of matter on arrested beams, i.e., a population at thermal equilibrium. However, Wentzel[21] has made a theoretical calculation which shows that the effect is expected to be small unless the tau has a high anomalous magnetic moment. In any event, the result of this test must be positive in order to be significant.

The phase space foe Eulerian angles is $d \cos \Theta \, d\Phi \, d\Psi$, therefore Figs. 11, 12, and 13 show histograms of number vs $\cos \Theta$, Φ, and Ψ, respectively. Examination of these histograms reveals no serious deviation from isotropy, which is the expected distribution in case there is no polarization. The probability that the distribution in $\cos \Theta$ and Φ is due to random fluctuations from isotropy was obtained by a χ^2 test as 10%.

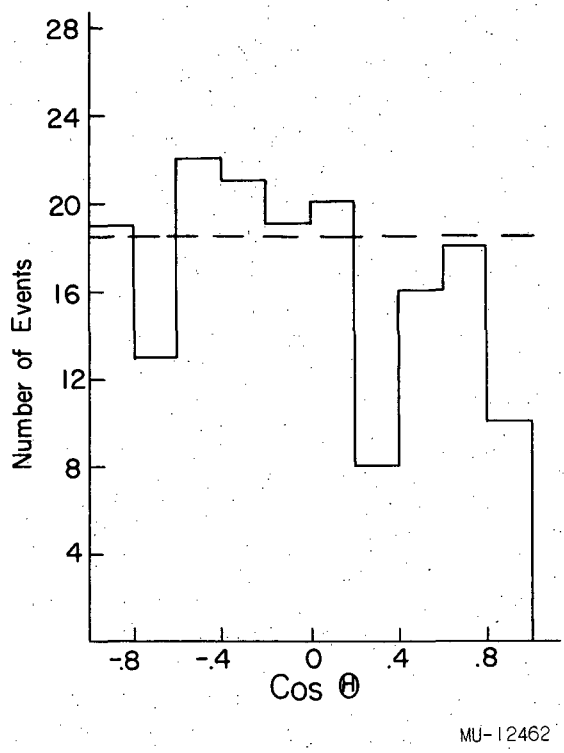

Fig. 11. Histogram of number vs cos Θ, where Θ is the polar angle of the normal to the decay plane. The horizontal line is the expected curve if there is no polarization.

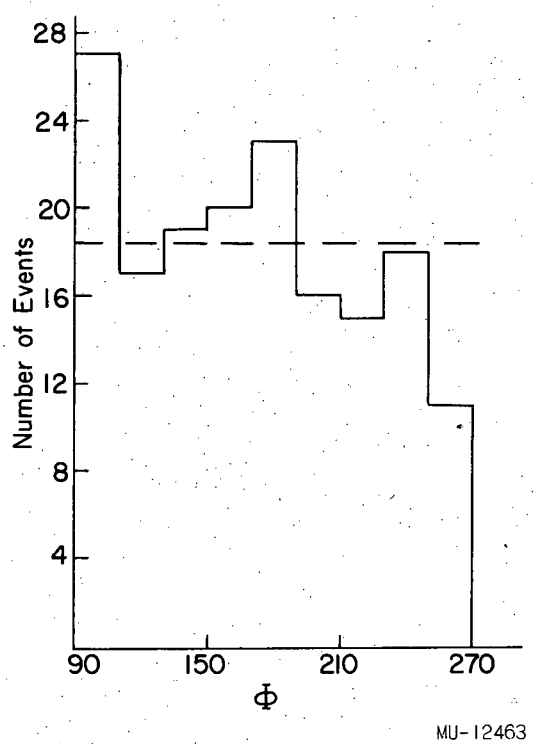

Fig. 12. Histogram of number vs ϕ, where ϕ is the azimuthal angle of the normal to the decay plane. The horizontal line is the expected curve if there is no polarization.

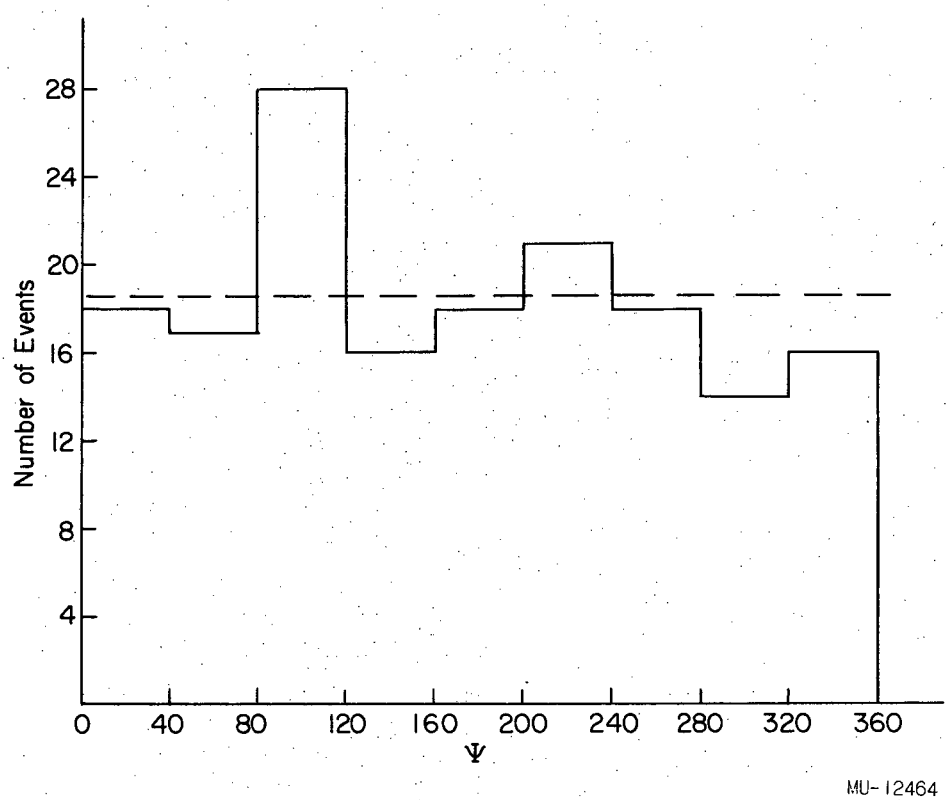

Fig. 13. Histogram of number vs ψ, where ψ is the Eulerian angle which defines the direction of the odd pion in the decay plane. The horizontal line is the expected curve if there is no polarization.

VII. SUMMARY OF CONCLUSIONS

A mass for the tau meson of 966.5 ± .74 electron masses was found by summing the total energies of its three decay pions. Petersen, who used the same sample of taus, found a mass of 966.3 ± 1.9 electron masses by the range-momentum method.[3] These results indicate that for the tau meson, at least, there is no significant difference between its "primary" mass and its "secondary" mass and any proposal to explain the apparent mass degeneracy of the τ and θ must be reconciled with this fact. This means, for example, in the genetic scheme of Lee and Orear[25] and Treiman and Wyd,[24] that the tau decay does not result from a (0, 0) transition of the θ because this transition requires about 15 Mev mass difference.

The energy spectrum and angular distribution of the pions from the tau decay, when compared with the Dalitz analysis, indicate that the tau has a spin-parity incompatible with that of the θ, and furthermore, these distributions agree quite well with those derivable purely from phase space. These conclusions do not suffer from the objections raised against previous results that (a) a scanning bias for low-energy pions exists, (b) there is a bias which arises from restriction of certain decay configuration by too-small stack dimensions, (c) relativistic effects are not considered. The statistics are still to meager to permit a final decision on the spin-parity of the tau; however, the negative results of a search for possible polarization effects do not contradict the possibility that the tau is pseudoscalar.

ACKNOWLEDGMENTS

I should like to express my appreciation of the continued support and friendly council of Professor Chaim Richman during the years of my graduate work. It is a further pleasure to express my deep gratitude to Dr. Robert W. Birge, Dr. Donald H. Stork, and Dr. Marian Whitehead for their many contributions and helpful suggestions throughout the course of this work; and to Dr. James R. Petersen, Mr. Leroy T. Kerth, and Mr. Jack Sandweiss for many constructive criticisms in connection with this analysis. Many questionable points in connection with the Dalitz theory were clarified as a results of discussions with Dr. Dan H. Holland. I am deeply indebted to Mr. Victor Cook for his invaluable help with the measurements and computations. I thank Mr. Robert Fry, Mr. George Preston, and Mr. Thomas Reynolds for their assistance with the measurements; Mr. James Baker for help with the portions of this work done on the IBM-650 computing machine; and the scanners, Mrs. Beverly Baldridge, Miss Irene d'Arche, Mrs. Edith Goodwin, Mrs. Marilynn Harbert, and Miss Kathryn Palmer. Without the Kerth-Stork spectrometer, the experiment would have been impossible.

I am very grateful to Dr. Edward J. Lofgren and the Bevatron crew for providing the successful exposure of the emulsion stack.

Further, I welcome this opportunity to acknowledge my indebtedness to many others--above all my wife, Pat--for their help and forbearance.

This work was done under the auspices of the United States Atomic Energy Commission.

APPENDICES

A. Direction-Cosine Errors

A-1. Derivation of Direction-Cosine Errors Due to Measurement Errors and Multiple Coulomb Scattering

The measured quantities are θ, the angle of the track to the x axis of the microscope system; the length ρ of the track in the plane of the emulsion; and the rise of the track, Δz. In terms of these the direction cosines relative to the Bevatron coordinate system (Fig. 1) are:

$$\alpha = \rho \frac{\cos\theta}{R}, \quad \beta = \frac{\Delta z}{R}, \quad \alpha = \rho \frac{\sin\theta}{R}, \tag{1}$$

where

$$R = \sqrt{\rho^2 + \Delta z^2}; \quad \rho = fr; \quad \Delta z = s\Delta z'; \quad s = \frac{\bar{t}_b}{\bar{t}_a}. \tag{2}$$

The multiplicative constants f and s convert from reticle units to microns and from postdevelopment to predevelopment dimensions, respectively. The standard deviations of the variables ρ, θ, Δz due to measurement errors are

$$\begin{aligned} S_\theta, S\rho/\rho &= \sqrt{S_r^2/r^2 \quad S_f^2/f^2}, \\ S_{\Delta z}/\Delta z &= \sqrt{S_{\Delta z'}^2/\Delta z' + S_s^2/s^2}. \end{aligned} \tag{3}$$

Propagating these errors through the expressions for the direction cosines, by the usual method, we obtain

$$
\begin{aligned}
S_\alpha^{\ 2} &= \gamma^2 S_\theta^{\ 2} + \alpha^2 \beta^4 F^2 , \\
S_\beta^{\ 2} &= \beta^2 (1 - \beta^2)^2 F^2 , \\
S_\gamma^{\ 2} &= \alpha^2 S_\theta^{\ 2} + \gamma^2 \beta^4 F^2 , \\
F^2 &= S_\rho^{\ 2}/\rho^2 + S_{\Delta z}^{\ 2}/\Delta z^2 = S_r^{\ 2}/f^2 + S_{\Delta z'}^{\ 2}/\Delta z'^2 + \\
&\qquad S_f^{\ 2}/f^2 + S_s^{\ 2}/s^2 .
\end{aligned}
\tag{4}
$$

For stacks No. 16 and No. 20 the normals to the emulsion sheets were along the y axis of the Bevatron system; we set up a new coordinate system with polar axis along the y axis of the Bevatron; in terms of this system we have

$$\alpha = \sin \theta' \sin \phi', \ \beta = \cos \theta', \ \gamma = \sin \theta' \cos \phi' , \tag{5}$$

where θ' is the polar angle and ϕ' the azimuthal angle. Now, multiple scattering out of the plane of the emulsion produces an error in θ' which for a track of length R (microns) and kinetic energy T (in Mev) is

$$S_{\theta'} = \sqrt{\overline{\theta_x^{\ 2}}} = \sqrt{3/2} \ /180 \ K/2T \ (R/100)^{1/2} \text{ radians}, \tag{6}$$

where K is assumed to be 27 degree-Mev/100 microns. Here $\sqrt{\overline{\theta_x^{\ 2}}}$ is the rms projected scattering angle. Then we have

$$S_\alpha = \frac{\alpha\beta}{\sqrt{1-\beta^2}} \sqrt{\overline{\theta_x^{\ 2}}} , \quad S_\beta = \sqrt{1-\beta^2} \sqrt{\overline{\theta_x^{\ 2}}} , \quad S_\gamma = \frac{\beta\gamma}{\sqrt{1-\beta^2}} \sqrt{\overline{\theta_x^{\ 2}}} . \tag{7}$$

Finally, the error in direction cosines due both to measurement errors and multiple scattering is

$$
\begin{aligned}
S_\alpha^{\ 2} &= \gamma^2 S_\theta^{\ 2} + \alpha^2 \beta^4 F^2 + \frac{\alpha^2\beta^2}{1-\beta^2} \overline{\theta_x^{\ 2}} , \\
S_\beta^{\ 2} &= \beta^2 (1-\beta^2)^2 F^2 + (1-\beta^2) \overline{\theta_x^{\ 2}} , \\
S_\gamma^{\ 2} &= \alpha^2 S_\theta^{\ 2} \gamma^2 \beta^4 F^2 + \frac{\beta^2\gamma^2}{1-\beta^2} \overline{\theta_x^{\ 2}} , \\
F^2 &= S_\rho^{\ 2}/\rho^2 + S_{\Delta z}^{\ 2}/\Delta z^2 = S_r^{\ 2}/r^2 + S_{\Delta z'}^{\ 2}/\Delta z'^2 + S_f^{\ 2}/f^2 + S_s^{\ 2}/s^2 .
\end{aligned}
\tag{8}
$$

A-2. Effect of Direction-Cosine Errors on Coplanarity

The unit radius vectors of the three pions are

$$\vec{a} = \alpha_1 \vec{i} + \beta_1 \vec{j} + \gamma_1 \vec{k},$$
$$\vec{b} = \alpha_2 \vec{i} + \beta_2 \vec{j} + \gamma_2 \vec{k}, \tag{9}$$
$$\vec{c} = \alpha_3 \vec{i} + \beta_3 \vec{j} + \gamma_3 \vec{k}.$$

In terms of these the normals to alternate pairs of pions are given by

$$\vec{A} = \vec{b} \times \vec{c}, \quad \vec{B} = \vec{c} \times \vec{a}, \quad \vec{C} = \vec{a} \times \vec{b}, \tag{10}$$

and the angle δ, which is included between the normal to two of the pions and the third pion, may be taken to be

$$\cos \delta = \frac{\vec{C} \cdot \vec{c}}{C\ C} = \frac{\vec{C} \cdot \vec{c}}{C} . \tag{11}$$

Then an error in $\cos \delta$ is

$$d \cos \delta = \frac{d\vec{C} \cdot \vec{c}\, \vec{C} \cdot \vec{dc} - \vec{C} \cdot \vec{c}\,(dC/C + dc/c)}{C}, \tag{12}$$

where $d\vec{C} = d(\vec{a} \times \vec{b}) = \vec{da} \times \vec{b} + \vec{a} \times \vec{db}$
and $\vec{da} = d\alpha\, \vec{i} + d\beta_1\, \vec{j} + d\gamma_1\, \vec{k}$, and similarly for $\vec{db}$ and $\vec{dc}$.
Putting in $\vec{a}, \vec{b}, \vec{c}, \vec{da}, \vec{db}, \vec{dc}$ explicitly and rearranging terms, one obtains

$$\begin{aligned} d \cos \delta = \Big\{ & A_x\, d\alpha_1 + A_y\, d\beta_1 + A_Z\, d\gamma_1 \\ & - B_x\, d\alpha_2 - B_y\, d\beta_2 - B_Z\, d\gamma_2 \\ & + C_x\, d\alpha_3 + C_y\, d\beta_3 + C_z\, d\gamma_3 \Big\}^{1/2} / C , \end{aligned} \tag{13}$$

from which it easily follows that we have

$$S \cos \delta = 1/C \left\{ A_x^2 S\alpha_1^2 + A_y^2 S\beta_1^2 + A_Z^2 S\gamma_1^2 + B_x^2 S\alpha_2^2 + B_y^2 S\beta_2^2 + B_Z^2 S\gamma_2^2 + C_x^2 S\alpha_3^2 + C_y^2 S\beta_3^2 + C_z^2 S\alpha_3^2 \right\}^{1/2} \tag{14}$$

$$= S/C ,$$

and $$\cos \delta / S \cos \delta = \frac{\vec{a} \times \vec{b} \cdot \vec{c}}{S} . \tag{15}$$

The quantity $\cos \delta / S \cos \delta$ was computed for each tau, for which measurement of direction cosines was possible, using the IBM-650 computing machine. These data are presented in column 16 of Appendix IV, and Fig. 3 shows the distribution of $\cos \delta / S \cos \delta$.

A-3. Effect of Direction-Cosine and Energy Errors on Momentum Balance

The momentum unbalance along each coordinate axis is Δp_x, Δp_y, Δp_Z, and the total unbalance is Δp:

$$\Delta p_x = \sum_{i=1}^{3} p_i \alpha_i ,$$

$$\Delta p_y = \sum_{i=1}^{3} p_i \beta_i , \tag{16}$$

$$\Delta p_Z = \sum_{i=1}^{3} p_i \gamma_i ,$$

$$\Delta p = \sqrt{\Delta p_x^2 + \Delta p_y^2 + \Delta p_X^2} .$$

Propagating the direction cosine and energy errors through these expressions, one obtains

$$S_{\Delta p_x}{}^2 = \sum_{i=1}^{3} \alpha_i{}^2 S_{p_i}{}^2 + p_i{}^2 S\alpha_i{}^2 ,$$

$$S_{\Delta p_y}{}^2 = \sum_{i=1}^{3} \beta_i{}^2 S_{p_i}{}^2 + p_i{}^2 S\beta_i{}^2 ,$$

$$S_{\Delta p_Z}{}^2 = \sum_{i=1}^{3} \alpha_i{}^2 S_{p_i}{}^2 + \rho_i{}^2 S_{\alpha_i}{}^2 , \tag{17}$$

$$S^2{}_{\Delta p} = [\Delta p_x{}^2 S_{\Delta p_x}{}^2 + \Delta p_y{}^2 \Delta p_y{}^2 + \Delta p_Z{}^2 S_{\Delta p_Z}{}^2]/\Delta p^2$$

The percent error in energy, S_T/T, varies by 16% over the energy interval considered, but for the purpose of this computation was assumed to be a constant. Then, $\frac{S_p}{p} = \frac{1}{2}\frac{S_T}{T}$ is about 8%. The quantities $\Delta p_x/S_{\Delta p_x}$, $\Delta p_y/S_{\Delta p_y}$, $\Delta p_Z/S_{\Delta p_Z}$, $\Delta p/S_{\Delta p}$ were computed for each tau that had all three pions stopping in the stacks with none of the pions making a large-angle scatter, by use of an IBM-650 computing machine. Column 15 of Appendix IV gives $\Delta p/S_{\Delta p}$ for individual taus. Figures 4 and 5 show the distributions of $\Delta p_x/S_{\Delta p_x}$ and $\Delta p/S_{\Delta p}$, respectively.

B. Humidity Error

The error in Q due to an error in estimating the emulsion density as $\rho_E = 3.826\ g/cm^3$ arises strictly from the difference in water content between the assumed and true values of the emulsion density. To estimate the effect of this error:

1. R_i, Z_i, R_{E_i}, Z_{E_i} are defined in Section III-B-2a. R_{t_i} is is the chord length for the true emulsion density ρ_t.
2. As in Section III-B-2a, we have
   $R_{E_i}/R_i = Z_{E_i}/Z_i$, $R_{t_i}/R_i = Z_{t_i}/Z_i$ and $\rho_t = \sigma = \rho_E t_E = \rho_t t_t$.
   Now we see $R_{E_i}/R_{t_i} = Z_{E_i}/Z_{t_i} \simeq t_E/t_t = \rho_t/\rho_E$,
   from which follows
   $$\sum_i R_{E_i} \simeq \rho_t/\rho_E \sum_i R_{t_i} \quad \text{or} \quad R_E \simeq p_t/p_E\ R_t .$$
3. $dT/dx = \text{const} \times n \times f(v)$, where n is the number of electrons per unit volume of emulsion. To within the accuracy of measurement the water and dry emulsion volumes are additive. Therefore n depends linearly on the emulsion density, i.e., $n = b\rho + d$. Barkas and Young[29] given $n = (0.2522\ \rho + 0.0830)\ 10^{24}/cm^3$ as the dependence of n on ρ. Now the range is
   $$R(T_0) = \int_0^{T_0} dT/(dT/dx) = \frac{1}{\text{const.} \times n} \int_0^{T_0} dT/f(v),$$
   $$\therefore\ nR = g(v)$$
   Assume for convenience that $T = a(Rn)^k$, where $k = \frac{1}{1.71}$. The range index k varies by about 14% over the region of interest; we have taken the mean value.
4. $T_t - T_E/T_E = \Delta T/T_E = (R_t n_t/R_E n_E)^k - 1 = (\rho_E n_t/\rho_t n_E)^k - 1.$

5. Assume $\rho_t = \rho_E + \Delta$ and make a Taylor's expansion of n_t/ρ_t about n_E/ρ_E. One obtains

$$n_t/\rho_t = n_E/\rho_E(1 - d\Delta\rho/n_E\rho_E).$$

Then we have

$$\Delta T/T_E = (1 - d\Delta\rho/n_E\rho_E)^k - 1 \simeq kd\,\Delta\rho/n_E\rho_E\ .$$

Putting in the values of k, d, and ρ_E given above, one obtains

$$\Delta T/T = -0.046\ \Delta\rho/\rho\ .$$

Then we have

$$\sum_{i=1}^{3} \Delta T_i = \Delta Q = \sum_{i=1}^{3} (-0.046)\ \frac{\Delta\rho}{\rho}\ T_i = Q\,(-0.046)\Delta\rho/\rho,$$

and

$$\Delta Q/Q = -0.046\ \Delta\rho/\rho\ .$$

C. Effect of Increasing the Interaction Radius

In the Dalitz analysis, increasing the interaction radius will necessitate consideration of terms of higher $\lambda = \ell + \ell'$. From Table III it is seen that λ increases by at least two from its minimum value when additional states are considered. For the low-spin unique cases, (1 +) and (2 +) have terns with λ two greater than minimum and (0 -), (1 -), and (3 -) have terms with λ four greater than minimum. We shall investigate the effect of increasing the interaction radius for (0 -) and (1 +), which typify the two situations.

In the expression for $c_{\ell\ell'}$ we rewrite the quantity $(m/M)^{\ell+\ell'}$ as $(R/\lambda\!\!\!^{-}\pi)^{\ell+\ell'}$, where R is the interaction radius and $\lambda\!\!\!^{-}\pi$ is the pion Compton wave length; then the expression for $c_{\ell\ell'}$ becomes

$$c_{\ell\ell'} = A_{JP}\ \frac{a_\lambda(\ell+1)!!\ (\ell'+1)!!}{(\lambda+4)!!(2\ell+1)!!(2\ell'+1)!!}\left(\frac{R}{\lambda\!\!\!^{-}\pi}\right)^{\lambda}\left(\frac{p}{m}\right)^{\ell}\left(\frac{p'}{m}\right)^{\ell'}.$$

In the following, the variables $q = p/p_{max}$, $q' = p'/p'_{max}$ are used where p_{max}, p'_{max} are the maximum values of p and p', respectively.

C-1. Case of (0 -)

The pairs (ℓ, ℓ') that may contribute to the matrix element for this case are (0, 0); (2, 2) · (4, 4); . . .; with corresponding λ of 0, 4, 8, ... The square of the matrix element for the terms $\lambda = 0$, 4 is

$$F_{O-} = 1 + K^2 q^4 q'^4 (3 \cos^2\theta_2 - 1)^2 + 2 K \cos\phi q^2 q'^2 (3 \cos^2\theta - 1),$$

$$K = 3/2\sqrt{5}\, p_{max}^2/M^2\, p'^2_{max}/M^2 \frac{(a_4/a_0)}{1200} (R/\lambda\!\!\!^{-})^4$$

$$= \frac{a_4/a_0 (R/\lambda\!\!\!^{-}\pi)^4}{1.9 \quad 10^5} .$$

The quantity a is a monotonically decreasing function of λ, but for the purposes of this calculation the ratio of a's will be taken to be unity. Estimating that K must be greater than 0.01 to show any effect, we obtain

$$(R/\lambda\!\!\!^{-}\pi)^4 \simeq 1.9 \times 10^3 ,$$

$$R/\lambda\!\!\!^{-}\pi \simeq 6.7.$$

C-2. Case of (1 +)

The paris (ℓ, ℓ') that may contribute to the matrix element for this case are (0, 1); (2, 1); · · · with corresponding λ of 1, 3, · · · . The square of the matrix element for the terms $\lambda = 1, 3$ is

$$F_{1+} = q'^2 + K^2 q'^2 q^4 - 2K \cos\phi\, q'^2 q^2 (2 \cos^2\theta - 1) ,$$

$$K = \frac{a_3/a_1}{3.81 \times 10^2} (R/\lambda\!\!\!^{-}\pi)^2 .$$

Again, letting $K = 0.01$ we have

$$a_3/a_1 = 1 ,$$

$$(R/\lambda\!\!\!^{-}\pi)^2 \simeq 3.8 ,$$

$$(R/\lambda\!\!\!^{-}\pi) \simeq 1.95;$$

for a $K = 0.05$ we have

$$a_3/a_1 = 1 ,$$

$$(R/\lambda\!\!\!^{-}\pi) \simeq 4.4 .$$

In this case it is conceivable that the effect of higher terms in λ may be felt if the interaction radius is about a pion Compton wave length.

D. Table of Original Data

Explanation of Table

Columns 1 and 2: Tau identification

Column 1 is the stack number and column 2 is the K-meson number in the stack. There were three stacks of 600-μ G.5 emulsion, numbered 16, 17, and 20. Stack No. 16 consisted of 105 pellicles 3.5 by 3.5 in. in area, stack No. 17 consisted of 40 pellicles 3 by 6 in. in area, and stack No. 20 consisted of 95 pellicles 9 by 17.5 in. in area. The nominal K-beam energy was 114 Mev for stacks No. 16 and No. 20 and 170 Mev for stack 17.

Column 3: Scanning

T.F. signifies scanning by systematic track-following.
S.A.S. signifies scanning by systematic area scanning.
N.S. signifies the tau was found nonsystematically. One found such taus while following a selected track, while following a secondary pion, or while relocating a tau. Stack No. 16 has significantly more nonsystematics because it was exposed twice and the tracks from the two exposures were at right angles.

Columns 4, 5, and 6: Pion energy

The a, b, or c before each energy indicates a designation of the pions between which the angles with cosines $\vec{a}\cdot\vec{b}$, $\vec{b}\cdot\vec{c}$, $\vec{c}\cdot\vec{a}$ are included.

Columns 7 and 8: Dalitz variables

The varible of Column 7 is $r = T_\pi \Big/ \left[T_\pi\right]_{max}$, where $\left[T_\pi\right]_{max} = \left(\frac{M_\tau + m_\pi}{2M_\tau}\right) Q$. The variable $\cos\theta$ is the cosine of the angle between the relative momentum of the like pions and the momentum of the unlike pion.

Columns 9, 10, and 11: Eulerian angles

The Eulerian angles Θ, Φ, and Ψ describe the orientation of the normal to the decay plane and the direction of the odd pion, where z is the normal to the production plane and positive upwards, x is along the τ-beam direction, y is the third member of a right-handed system, and z' is along the old pion direction.

Columns 12, 13, and 14: Angles between pions

These columns give the cosine of the angle between pions designated in columns 4, 5, and 6.

Column 15: Momentum unbalance

The ratio of the measured momentum unbalance (ΔP) to an estimated uncertainty in the momentum balance ($S\Delta P$) was computed for the taus having three pions stopping in stacks. The uncertainty in the momentum balance was computed by propagating measurement errors and range straggling through the momentum-balance equation. The same set of suitable averaged measurement errors was used in each computation.

In a few cases the tau decayed at the surface of an emulsion, hence one or more pions were not visible at the τ decay. For these cases the angles between pions could not be accurately estimated and momentum unbalance and coplanarity were not computed.

Column 16: Coplanarity

The angle δ is included between the normal to the plane containing two of the pions and the third pion. The uncertainty in $\cos\delta$--i.e., $S\cos\delta$--was computed as for momentum unbalance, and used the same set of measurement errors.

TABLE OF ORIGINAL DATA

(1) Stack Number	(2) Event Number	(3) Scan-ning	(4) Pion Energy (Mev) π^+	(5) π^+	(6) π^-	(7) r	(8) $\cos\theta$	(9) $\cos\Theta$	(10) Eulerian Angles Φ (deg)	(11) Ψ (deg)	(12) $\vec{a}\cdot\vec{b}$	(13) $\vec{b}\cdot\vec{c}$	(14) $\vec{c}\cdot\vec{a}$	(15) $\Delta P/S\Delta P$	(16) $\cos\delta/S\cos\delta$
16	5	T.F.	a 46.0	c 11.4	b 17.3	0.361	0.918	0.243	154	200	$\bar{0}$.9503	0.7309	$\bar{0}$.9065	1.09	0.59
16	7	T.F.	c 32.9	b 12.4	a 28.9	0.607	0.513	$\bar{0}$.0081	141	135	$\bar{0}$.2063	$\bar{0}$.4028	$\bar{0}$.8121	0.90	0.87
16	36	T.F.	c [45.4]	b 17.6	a 9.5	0.204	0.942	$\bar{0}$.0655	110	48.6	0.8901	$\bar{0}$.9785	$\bar{0}$.9646		0.77
16	40	T.F.	c 30.6	a 30.6	b 12.3	0.263	0.0185	0.0913	155	240	$\bar{0}$.2836	$\bar{0}$.3364	$\bar{0}$.8074	0.51	0.34
16	51	T.F.	c 32.7	a 15.7	b 25.5	0.538	0.427	$\bar{0}$.7345	119	185	$\bar{0}$.1714	$\bar{0}$.7779	$\bar{0}$.4852	1.19	0.60
16	85	T.F.	a 19.0	b 11.3	c 44.2	0.925	0.332	$\bar{0}$.2711	117	206	0.5966	$\bar{0}$.8448	$\bar{0}$.9329	0.91	0.50
16	86	N.S.	c 42.0	a 11.6	b 20.7	0.435	0.774				0.3347	$\bar{0}$.8751	$\bar{0}$.7487	1.36	0.24
16	103	T.F.	c 40.4	a 28.0	b 5.2	0.110	0.550	$\bar{0}$.1836	242	202	0.2818	$\bar{0}$.6227	$\bar{0}$.9256	1.68	0.80
16	123	T.F.	c 18.6	b 17.6	a 38.0	0.798	0.0296	$\bar{0}$.7002	240	101	$\bar{0}$.6808	0.0238	$\bar{0}$.7479	1.90	0.91
16	131	T.F.	a [46.2]	b 20.0	c 8.9	0.185	0.900	0.4019	115	326	$\bar{0}$.9635	0.8387	$\bar{0}$.9525		1.63
16	163	T.F.	c 39.3	b 19.6	a 15.0	0.316	0.558	0.1266	134	270	0.2713	$\bar{0}$.8415	$\bar{0}$.7481	1.67	0.06
16	181	T.F.	c 14.6	b 13.4	a 49.5	0.996	0.237	0.5022	248	11.1	$\bar{0}$.9691	0.9053	$\bar{0}$.9811	1.44	0.91
16	203	T.F.	a 39.5	b 17.5	c 18.2	0.377	0.579	0.3025	156	304	$\bar{0}$.7454	0.1190	$\bar{0}$.7503	1.64	0.49
16	219	T.F.	c 30.0	b 9.0	a 35.8	0.746	0.564	0.0618	211	217	$\bar{0}$.4142	$\bar{0}$.0635	$\bar{0}$.8819	0.41	0.14
16	236	T.F.	b 21.7	c 14.2	a 39.1	0.813	0.224	0.0776	257	86.5	$\bar{0}$.7987	0.0902	$\bar{0}$.6710	1.15	0.76
16	248	T.F.	c 42.2	b 21.6	a 11.6	0.240	0.635	0.6448	156	113	0.4108	$\bar{0}$.8914	$\bar{0}$.7783	0.91	1.00
16	273	T.F.	b 31.2	c 23.4	a 21.3	0.438	0.198	0.6969	179	12.1	$\bar{0}$.5744	$\bar{0}$.6540	$\bar{0}$.2433	1.71	0.22
16	279	T.F.	c 42.2	b 6.4	a 25.7	0.539	0.875	$\bar{0}$.7698	135	63.6	0.5915	$\bar{0}$.7890	$\bar{0}$.9619	1.36	0.27
16	298	T.F.	c 28.5	b 2.7	a 41.4	0.889	0.914	0.0894	162	87.0	$\bar{0}$.8914	0.8250	$\bar{0}$.9913	1.27	0.64
16	307	T.F.	a 35.3	b 21.4	c 17.6	0.369	0.374	$\bar{0}$.3436	161	273	$\bar{0}$.7543	$\bar{0}$.0136	$\bar{0}$.6455	1.21	0.68
16	308	N.S.	c 39.0	a 17.2	b 18.7	0.389	0.571				0.1677	$\bar{0}$.7420	$\bar{0}$.7848	1.59	0.64
16	311	T.F.	c 31.5	b 22.0	a 20.5	0.432	0.247	$\bar{0}$.9543	102	320	$\bar{0}$.2338	$\bar{0}$.6258	$\bar{0}$.6117	0.72	0.54
16	315	T.F.	c 18.6	b 14.5	a 40.9	0.862	0.139	$\bar{0}$.6994	104	117	$\bar{0}$.7559	0.2800	$\bar{0}$.8400	0.85	0.16
16	336	T.F.	c 41.3	b 13.9	a 20.0	0.415	0.700	0.5991	242	101	0.3464	$\bar{0}$.7958	$\bar{0}$.8436	1.12	0.29
16	338	T.F.	b 20.7	a 13.9	c 39.6	0.832	0.213	$\bar{0}$.5192	93.0	286	0.2376	$\bar{0}$.8309	$\bar{0}$.7378	0.18	0.00
16	349	N.S.	c 38.0	a 34.5	b 3.9	0.0796	0.175				$\bar{0}$.0155	$\bar{0}$.2503	$\bar{0}$.9640	1.20	0.71
16	397	T.F.	c 18.0	b 14.6	a [40.0]	0.859	0.116	$\bar{0}$.2710	99.7	234	$\bar{0}$.7691	0.3282	$\bar{0}$.8557		0.94
16	398	T.F.	c 33.0	b 15.7	a 24.6	0.523	0.439	$\bar{0}$.3516	130	258	$\bar{0}$.2193	$\bar{0}$.5454	$\bar{0}$.6980	1.86	0.04
16	405	T.F.	c [47.5]	b 13.3	a 13.5	0.283	0.991	0.9937	174	288	0.9786	$\bar{0}$.9932	$\bar{0}$.9955		0.57
16	431	T.F.	c 26.1	b 20.2	a 27.8	0.585	0.149	$\bar{0}$.9731	268	299	$\bar{0}$.4551	$\bar{0}$.3575	$\bar{0}$.6686	0.87	0.76

Stack Number	Event Number	Scan-ning	Pion Energy (Mev) π^+	π^+	π^-	r	$\cos\theta$	$\cos\Theta$	Eulerian Angles Φ (deg)	Ψ (deg)	$\vec{a}\cdot\vec{b}$	$\vec{b}\cdot\vec{c}$	$\vec{c}\cdot\vec{a}$	$\Delta P/S\Delta P$	$\cos\delta/S\cos\delta$
16	443	T.F.	b 42.0	c 11.9	a 20.9	0.436	0.762	0.9472	187	226	$\bar{0}.8884$	$\bar{0}.7357$	0.3422	1.07	0.66
16	451	T.F.	b 27.5	a 9.7	c [35.6]	0.762	0.501	0.2067	187	160	$\bar{0}.0030$	$\bar{0}.8642$	$\bar{0}.5002$		0.47
16	457	T.F.	a 29.5	b 26.8	c 18.4	0.384	0.072	$\bar{0}.2320$	127	157	$\bar{0}.7029$	$\bar{0}.3207$	$\bar{0}.4481$	0.66	0.09
16	458	T.F.	c [28.2]	b 23.0	a 26.3	0.529	0.126	$\bar{0}.1773$	233	292	$\bar{0}.4232$	$\bar{0}.4909$	$\bar{0}.5773$		2.17
16	477	T.F.	a [42.6]	b [30.8]	c 1.75	0.0370	0.875	0.6144	260	129	$\bar{0}.9933$	0.8246	$\bar{0}.8842$		0.17
16	494	T.F.	a out	c 6.6	b out						$\bar{0}.9078$	0.2949	$\bar{0}.6681$		
16	502	T.F.	a 36.0	c 20.2	b 17.8	0.375	0.424	$\bar{0}.2619$	91.2	349	$\bar{0}.6936$	0.0004	$\bar{0}.7200$	0.86	1.06
16	A-1	N.S.	c 30.2	a 12.3	b 31.4	0.663	0.459				$\bar{0}.2937$	$\bar{0}.8240$	$\bar{0}.2990$	1.05	0.43
16	A-2	N.S.	b 24.0	a 13.0	c 38.7	0.797	0.316				0.0889	$\bar{0}.8174$	$\bar{0}.6460$	1.51	0.39
16	A-3	N.S.	c 14.4	a 13.0	b [46.7]	0.983	0.121				$\bar{0}.9715$	$\bar{0}.9759$	0.8972		0.33
16	A-5	S.A.S.	c 43.1	a 4.9	b 25.9	0.546	0.934				0.5723	$\bar{0}.9720$	$\bar{0}.7478$	1.33	0.83
16	N1	T.F.	a 31.2	c 28.8	b 14.1	0.297	0.070	0.4672	266	160	$\bar{0}.3792$	$\bar{0}.3408$	$\bar{0}.7408$	1.88	0.57
16	N10	T.F.	c 34.6	a 8.8	b 32.5	0.668	0.641	$\bar{0}.5389$	238	99.5	$\bar{0}.8480$	$\bar{0}.8959$	$\bar{0}.3661$	1.36	0.50
16	N20	T.F.	a 38.3	c 16.9	b 19.5	0.407	0.555	$\bar{0}.1015$	150	194	$\bar{0}.7474$	0.0617	$\bar{0}.7090$	1.79	0.27
16	N23	T.F.	b 29.7	a 29.1	c 16.7	0.345	0.016	0.6641	142	287	$\bar{0}.7359$	$\bar{0}.3934$	$\bar{0}.3326$	0.58	0.45
16	N32	T.F.	c 19.6	b 17.5	a 38.2	0.791	0.060	0.8320	183	71.6	$\bar{0}.6793$	0.0871	$\bar{0}.7901$	2.29	0.39
16	N80	T.F.	c 43.7	a 16.4	b 13.0	0.277	0.814	0.2053	187	199	0.6216	$\bar{0}.8927$	$\bar{0}.9076$	1.14	0.57
16	N84	T.F.	a 43.0	b 23.0	c 9.8	0.202	0.659	0.6964	197	352	$\bar{0}.9285$	0.4365	$\bar{0}.7383$	1.42	0.92
16	N89	T.F.	c 20.1	a 12.2	b 43.1*	0.891	0.288	$\bar{0}.6265$	217	142	$\bar{0}.7991$	$\bar{0}.9043$	0.4671		0.81
16	N119	T.F.	b 37.6	a 7.9	c 30.2	0.622	0.723	0.9735	142	93.4	$\bar{0}.4845$	$\bar{0}.8944$	0.0582		
16	N129	T.F.	a 30.1	b 18.7	c 26.5	0.549	0.282	$\bar{0}.4340$	143	107	$\bar{0}.5100$	$\bar{0}.3188$	$\bar{0}.6525$	1.47	0.16
16	N145	T.F.	b 31.0	a 1.6	c 43.2	0.889	0.986	0.0820	107	348	0.8604	$\bar{0}.9959$	$\bar{0}.9029$	0.31	0.17
16	N149	T.F.	c 39.0	b 15.0	a 20.0	0.421	0.622	$\bar{0}.7528$	168	267	0.1471	$\bar{0}.6993$	$\bar{0}.8097$	0.90	0.28
16	N162	N.S.	a 36.0	b 36.0	c 1.9	0.040	0.000				$\bar{0}.9784$	0.0678	$\bar{0}.2724$	1.56	0.41
16	N194	T.F.	a 32.6	c 25.3	b 16.5	0.346	0.206	$\bar{0}.5807$	235	53.6	$\bar{0}.4585$	$\bar{0}.2711$	$\bar{0}.7310$	1.49	0.17
16	N197	T.F.	b 28.6	a 22.2	c 24.0	0.503	0.161	$\bar{0}.3012$	265	147	$\bar{0}.5112$	$\bar{0}.6461$	$\bar{0}.3255$	1.47	0.23
16	N210	T.F.	a 35.0	c 28.9	b 12.7	0.259	0.181	$\bar{0}.9729$	202	42.7	$\bar{0}.4878$	$\bar{0}.0974$	$\bar{0}.8211$	0.61	0.05
16	N214	T.F.	b 38.7	c 5.4	a 30.7	0.640	0.820	0.5753	243	166	$\bar{0}.9359$	$\bar{0}.4429$	0.1857	3.06	0.73
16	N225	T.F.	a [42.8]	c 3.4	b 26.6	0.570	0.973	$\bar{0}.5125$	231	39.5	$\bar{0}.9941$	0.8360	$\bar{0}.8899$		0.00
16	N241	T.F.	c 47.2	b 7.8	a 20.0	0.416	0.994	$\bar{0}.2578$	209	294	0.9952	$\bar{0}.9975$	$\bar{0}.9992$	0.59	0.63

Stack Number	Event Number	Scan-ning	Pion Energy (Mev) π^+	π^+	π^-	r	$\cos\theta$	Eulerian Angles $\cos\Theta$	ϕ (deg)	ψ (deg)	$\vec{a}\cdot\vec{b}$	$\vec{b}\cdot\vec{c}$	$\vec{a}\cdot\vec{c}$	$\Delta P/S\Delta P$	$\cos\delta/S\cos\delta$
17	1	N.S.	b 40.3	a 7.0	c 27.5	0.573	0.811				$\bar{0}$.5521	$\bar{0}$.9048	0.1452	1.60	2.05
17	7	N.S.	a [38.7]	b 25.9	c 11.1	0.229	0.402				$\bar{0}$.8774	0.1152	$\bar{0}$.5773		
17	40	T.F.	a [28.7]	b 20.0	c 21.0	0.556	0.215				$\bar{0}$.4343	$\bar{0}$.3840	$\bar{0}$.6643		0.88
17	42	T.F.	a [35.1]	b 27.0	c 14.5	0.295	0.229				$\bar{0}$.7867	$\bar{0}$.1266	$\bar{0}$.5127		0.35
17	47	T.F.	b 42.7	a 17.0	c 15.8	0.326	0.703				$\bar{0}$.8333	$\bar{0}$.8388	0.3984	0.87	0.09
17	90	T.F.	c [46.3]	a 9.5	b 20.0	0.411	0.926				0.7815	$\bar{0}$.9670	$\bar{0}$.9141		0.56
17	97	T.F.	c [31.2]	b 14.5	c 30.0	0.618	0.413				$\bar{0}$.3353	$\bar{0}$.3490	$\bar{0}$.7656		0.48
17	115	T.F.	c 45.7*	a 7.1	b 21.8	0.456	0.959				0.8406	$\bar{0}$.9765	$\bar{0}$.9373		0.35
17	145	T.F.	c 29.3	a 24.5	b 20.5	0.430	0.125				$\bar{0}$.3293	$\bar{0}$.5106	$\bar{0}$.6434	0.44	0.17
17	152	T.F.	c 20.2	a 8.4	b [45.0]	0.953	0.622				$\bar{0}$.9188	$\bar{0}$.9729	0.8030		0.15
17	170	N.S.	c 34.9	b 16.8	a 24.0	0.494	0.448				$\bar{0}$.1289	$\bar{0}$.5798	$\bar{0}$.7329	0.77	0.11
17	187	N.S.	a 40.5	c 16.5	b 18.5	0.382	0.626				$\bar{0}$.7987	0.2488	$\bar{0}$.7812	0.45	0.37
17	188	T.F.	a [34.5]	b 26.4	c 18.1	0.357	0.209				$\bar{0}$.7375	$\bar{0}$.1989	$\bar{0}$.5147		0.64
17	193	T.F.	a 43.2	c 9.0	b 22.3	0.467	0.852				$\bar{0}$.9287	0.5453	$\bar{0}$.8165	1.02	0.73
17	204	T.F.	b 19.3	a 12.1	c [45.5]	0.923	0.299				0.6067	$\bar{0}$.9100	$\bar{0}$.8814		0.24
17	215	T.F.	a [40.0]	b 22.0	c 11.2	0.239	0.571				$\bar{0}$.8724	0.3113	$\bar{0}$.7352		0.91
20	111	T.F.	b 20.2	c 20.1	a 36.2	0.738	0.003	$\bar{0}$.6223	177	57.8	$\bar{0}$.6802	$\bar{0}$.0788	$\bar{0}$.6759	1.53	1.35
20	125	T.F.	c 35.0	a 1.0	b 39.5	0.816	0.957	$\bar{0}$.3406	141	139	$\bar{0}$.4366	$\bar{0}$.9911	0.3139	0.78	0.30
20	165	T.F.	c 24.5	b 7.4	a [43.2]	0.897	0.625	$\bar{0}$.9275	183	59.3	$\bar{0}$.7806	0.5496	$\bar{0}$.9508		0.56
20	185	T.F.	c 28.2	b 6.9	a 39.8	0.829	0.641	$\bar{0}$.4729	143	191	$\bar{0}$.5718	0.1995	$\bar{0}$.9175	1.03	0.67
20	198	T.F.	b 32.2	c 14.5	a [26.2]	0.560	0.450	$\bar{0}$.8237	159	209	$\bar{0}$.7822	$\bar{0}$.4807	$\bar{0}$.1696		0.79
20	200	T.F.	c 29.7	b 2.9	a 41.6	0.874	0.888	0.6704	215	105	$\bar{0}$.7760	0.6036	$\bar{0}$.9310	1.79	0.38
20	233	T.F.	b 44.2	c 21.2	a 10.8	0.221	0.725	0.1182	208	24.3	$\bar{0}$.7868	$\bar{0}$.9118	0.4648	1.76	0.60
20	268	T.F.	a 35.0	c 33.0	b 7.0	0.146	0.077	$\bar{0}$.0476	225	199	$\bar{0}$.3193	$\bar{0}$.1144	$\bar{0}$.9048	0.51	0.03
20	270	T.F.	c 33.8	a 28.1	b 13.0	0.271	0.170	$\bar{0}$.1965	131	172	$\bar{0}$.1828	$\bar{0}$.4226	$\bar{0}$.8136	0.93	0.12
20	274	T.F.	b [45.1]	c 18.0	a 10.8	0.228	0.864	$\bar{0}$.3044	262	12.2	$\bar{0}$.9162	$\bar{0}$.9494	0.7447		0.36
20	283	T.F.	a 22.8	b 18.9	c 32.2	0.679	0.102	$\bar{0}$.5687	229	15.2	$\bar{0}$.1845	$\bar{0}$.5877	$\bar{0}$.6868	0.71	0.62
20	297	T.F.	a 39.0	c 9.0	b 26.0	0.549	0.742	0.0664	122	268	$\bar{0}$.9044	0.2821	$\bar{0}$.6641	1.23	0.48
20	307	T.F.	a 26.6	b 3.45	c [44.7]	0.932	0.967	0.1391	265	150	$\bar{0}$.9535	$\bar{0}$.9828	$\bar{0}$.9920		0.12

Stack Number	Event Number	Scan-ning	Pion Energy (Mev) π^+	π^+	π^-	r	$\cos\theta$	$\cos\Theta$	Eulerian Angles Φ (deg)	Ψ (deg)	$\vec{a}\cdot\vec{b}$	$\vec{b}\cdot\vec{c}$	$\vec{a}\cdot\vec{c}$	$\Delta P/S\Delta P$	$\cos\delta/S\cos\delta$
20	383	T.F.	c 46.0	a 18.6	b 10.8	0.223	0.8655	$\bar{0}.5705$	152	116	0.7592	$\bar{0}.9179$	$\bar{0}.9544$	0.82	0.86
20	393	T.F.	c 40.5	b 21.1	a 14.4	0.295	0.549	$\bar{0}.4061$	173	18	0.2310	$\bar{0}.8347$	$\bar{0}.7279$		0.77
20	397	T.F.	c 38.0	b 19.3	a 15.5	0.332	0.528	$\bar{0}.9858$	188	102	0.1918	$\bar{0}.7953$	$\bar{0}.7472$	0.59	0.29
20	408	T.F.	a 37.2	b 1.3	c 37.0	0.764	0.941	$\bar{0}.0510$	198	244	0.1792	$\bar{0}.3742$	$\bar{0}.9441$	0.96	0.59
20	420	T.F.	a 40.2	c 32.2	b 3.5	0.072	0.423	$\bar{0}.9952$	102	348	$\bar{0}.5576$	0.3278	$\bar{0}.9669$	0.46	0.71
20	446	T.F.	b 32.4	c 27.1	a 15.0	0.314	0.150	0.0534	216	90	$\bar{0}.4474$	$\bar{0}.7757$	$\bar{0}.2170$	0.85	0.31
20	480	T.F.	c 20.7	b 19.7	a 34.5	0.718	0.027	$\bar{0}.5141$	216	73	$\bar{0}.6922$	$\bar{0}.0780$	$\bar{0}.6648$	1.25	1.09
20	497	T.F.	b 36.5	a 1.6	c [36.4]	0.762	0.926	$\bar{0}.5705$	219	327	$\bar{0}.1052$	$\bar{0}.9772$	$\bar{0}.6792$		0.00
20	506	T.F.	c 34.7	a 23.2	b 17.8	0.367	0.305	$\bar{0}.5203$	164	116	$\bar{0}.1385$	$\bar{0}.6037$	$\bar{0}.7052$	1.25	1.25
20	518	T.F.	c [44.8]	a 9.8	b 17.9	0.385	0.935	0.7436	115	294	0.8188	$\bar{0}.9726$	$\bar{0}.9296$		0.28
20	534	T.F.	a 31.9	b 5.2	c 37.7	0.786	0.741	$\bar{0}.2355$	203	1	0.0824	$\bar{0}.4196$	$\bar{0}.9389$	0.59	0.51
20	552	T.F.	c 41.6	a 20.2	b 13.3	0.276	0.626	0.8850	181	163	0.3528	$\bar{0}.7650$	$\bar{0}.8721$	0.94	0.59
20	574	T.F.	b 35.7	c 4.8	a 34.9	0.722	0.790	0.6910	109	276	$\bar{0}.9384$	$\bar{0}.1661$	$\bar{0}.1839$	1.43	0.90
20	644	T.F.	c 39.3	a 8.6	b 27.0	0.562	0.749	0.7637	185	203	0.1793	$\bar{0}.8885$	$\bar{0}.6104$	1.03	0.28
20	699	T.F.	a 31.0	b 6.3	c 37.0	0.776	0.685	0.1084	147	332	0.1143	$\bar{0}.4695$	$\bar{0}.9302$	0.89	0.67
20	703	T.F.	c 34.1	a 5.9	b 36.0	0.739	0.730	$\bar{0}.8660$	138	173	$\bar{0}.2667$	$\bar{0}.9085$	$\bar{0}.1596$	1.09	0.46
20	707	T.F.	c [33.3]	a 7.0	b 37.4	0.751	0.678	$\bar{0}.4393$	155	101	$\bar{0}.3519$	$\bar{0}.9055$	$\bar{0}.0785$		0.06
20	734	T.F.	c 24.8	b 6.4	a 42.0	0.895	0.679	$\bar{0}.5136$	208	36	$\bar{0}.7932$	0.5735	$\bar{0}.9536$	0.52	0.44
20	749	T.F.	b [41.7]	c 16.2	a 15.3	0.326	0.718	0.0341	106	13	$\bar{0}.8508$	$\bar{0}.8467$	0.4410		
20	753	T.F.	a 41.8	c 15.5	b 18.1	0.374	0.690	$\bar{0}.1405$	213	1	$\bar{0}.8426$	0.3548	$\bar{0}.8002$	1.71	1.63
20	757	T.F.	c 24.2	b 21.8	a 27.0	0.577	0.061	$\bar{0}.2415$	144	177	$\bar{0}.4850$	$\bar{0}.4039$	$\bar{0}.6035$	1.16	0.53
20	759	T.F.	a 45.8	c 13.2	b 17.5	0.357	0.851	$\bar{0}.2734$	243	26	$\bar{0}.9085$	0.6052	$\bar{0}.8821$	0.61	0.35
20	768	T.F.	b 33.0	c 26.0	a 16.0	0.333	0.193	$\bar{0}.9389$	161	84	$\bar{0}.5094$	$\bar{0}.7657$	$\bar{0}.1622$	0.77	0.16
20	794	T.F.	b 38.2	c 26.6	a 10.5	0.217	0.374	0.3239	267	186	$\bar{0}.5538$	$\bar{0}.8590$	0.0496	0.52	0.11
20	859	T.F.	c 35.8	b 10.9	a 29.2	0.600	0.607	0.6918	234	254	$\bar{0}.0800$	$\bar{0}.4356$	$\bar{0}.8620$	1.07	1.12
20	860	T.F.	a [39.9]	c 11.7	b 22.8	0.478	0.706	0.8541	238	97	$\bar{0}.8297$	0.2506	$\bar{0}.7041$		0.72
20	966	T.F.	b 35.0	c 17.0	a 21.6	0.458	0.463	$\bar{0}.0134$	169	241	$\bar{0}.7354$	$\bar{0}.6649$	$\bar{0}.0169$	1.43	0.60
20	967	T.F.	a [39.6]	b 17.6	c 16.3	0.346	0.607	$\bar{0}.9167$	148	110	$\bar{0}.8174$	0.2579	$\bar{0}.7676$		0.44
20	994	T.F.	b 36.0	c 21.6	a 16.1	0.341	0.400	0.5092	184	254	$\bar{0}.6542$	$\bar{0}.7737$	0.0286	1.43	1.15
20	1001	T.F.	a 27.0	b 11.8	c 33.6	0.724	0.415	$\bar{0}.9634$	118	106	$\bar{0}.1546$	$\bar{0}.4551$	$\bar{0}.8091$	0.88	0.51

Stack Number	Event Number	Scan-ning	Pion Energy (Mev) π^+	π^+	π^-	r	cosθ	cosO	Eulerian Angles ϕ (deg)	ψ (deg)	$\vec{a}\cdot\vec{b}$	$\vec{b}\cdot\vec{c}$	$\vec{a}\cdot\vec{c}$	$\Delta P/S\Delta P$	cosδ/Scosδ
20	1009	T.F.	c 29.3	b 2.6	a 42.6	0.892	0.929	$\bar{0}$.2599	106	274	$\bar{0}$.7908	0.6624	$\bar{0}$.9822		
20	1016	T.F.	c 36.8	b 16.2	a 21.3	0.447	0.526	0.1276	120	272	0.0299	$\bar{0}$.6779	$\bar{0}$.7545		
20	1021	T.F.	b 23.9	a 21.2	c 30.8	0.633	0.067	$\bar{0}$.8191	156	166	$\bar{0}$.3088	$\bar{0}$.6328	$\bar{0}$.5409	0.37	0.02
20	1024	T.F.	b 24.8	a 15.1	c 36.3	0.743	0.259	$\bar{0}$.8084	266	89	$\bar{0}$.0258	$\bar{0}$.7942	$\bar{0}$.5866	0.56	0.22
20	1111	T.F.	c 39.3	b [21.9]	a 14.9	0.305	0.486	$\bar{0}$.1236	221	263	0.1623	$\bar{0}$.8212	$\bar{0}$.6962		0.09
20	1126	T.F.	b 29.3	a 7.2	c 38.9	0.804	0.633	0.8633	100	137	0.0482	$\bar{0}$.9207	$\bar{0}$.4337	1.71	0.32
20	1139	T.F.	c 35.8	b 22.9	a 15.0	0.317	0.367	$\bar{0}$.6282	176	268	$\bar{0}$.0467	$\bar{0}$.7540	$\bar{0}$.6198	1.19	1.10
20	1143	T.F.	a 25.7	b 5.0	a [45.0]	0.927	0.848	0.5864	100	145	0.8004	$\bar{0}$.8979	$\bar{0}$.9824		0.06
20	1145	T.F.	c [32.3]	b 13.9	a 29.0	0.601	0.456	$\bar{0}$.4724	109	213	$\bar{0}$.2448	$\bar{0}$.4023	$\bar{0}$.7874		
20	1156	T.F.	b 29.7	a 2.2	c [42.1]	0.887	0.945	0.8968	177	92	0.7796	$\bar{0}$.9903	$\bar{0}$.8584		0.13
20	1166	T.F.	a 36.8	b 6.7	c 30.3	0.640	0.754	$\bar{0}$.7456	192	166	$\bar{0}$.4126	0.0225	$\bar{0}$.9193		
20	1170	T.F.	c 29.3	b 27.6	a 18.3	0.379	0.045	$\bar{0}$.1058	197	206	$\bar{0}$.3524	$\bar{0}$.6916	$\bar{0}$.4312	1.21	1.22
20	1172	T.F.	b [36.6]	a 36.1	c 2.35	0.050	0.032	0.4740	143	106	$\bar{0}$.9697	$\bar{0}$.1597	$\bar{0}$.0861		0.31
20	1201	T.F.	a 37.2	c 14.4	b 24.3	0.499	0.560	0.7858	154	26	$\bar{0}$.7872	$\bar{0}$.0496	$\bar{0}$.5762	0.96	0.56
20	1204	T.F.	b 27.2	a 9.9	c 37.8	0.787	0.490	$\bar{0}$.8307	195	153	0.1335	$\bar{0}$.8801	$\bar{0}$.5875	1.00	0.51
20	1218	T.F.	a [39.5]	b 13.7	c 19.7	0.421	0.676	$\bar{0}$.0523	236	53	$\bar{0}$.7467	0.2781	$\bar{0}$.8464		0.41
20	1231	T.F.	b 34.2	a 19.5	c 17.9	0.390	0.403	$\bar{0}$.7642	126	101	$\bar{0}$.7359	$\bar{0}$.6805	$\bar{0}$.0049	1.05	0.04
20	1232	T.F.	c 20.5	a 12.8	b 43.0	0.879	0.266	$\bar{0}$.0443	220	349	$\bar{0}$.7499	$\bar{0}$.8583	0.3044	1.52	0.14
20	1239	T.F.	c 29.7	b 6.0	a 37.5	0.799	0.688	0.0055	119	249	$\bar{0}$.5365	0.1931	$\bar{0}$.9312	1.39	0.89
20	1282	T.F.	c 24.7	b 10.9	a 39.5	0.820	0.414	0.4008	122	217	$\bar{0}$.6646	0.2080	$\bar{0}$.8689	0.36	0.25
20	1287	T.F.	c 17.2	b 12.5	a 43.6	0.927	0.209	$\bar{0}$.3797	220	295	$\bar{0}$.8644	0.5795	$\bar{0}$.9090	0.51	0.03
20	1318	T.F.	b 39.5	c 27.1	a 7.6	0.160	0.462	$\bar{0}$.3291	196	216	$\bar{0}$.5785	$\bar{0}$.8989	0.1639	0.21	0.89
20	1339	T.F.	b 40.0	a 19.7	c 14.7	0.308	0.576	$\bar{0}$.1264	188	158	$\bar{0}$.8472	$\bar{0}$.7705	0.3144	1.43	0.19
20	1382	T.F.	c 42.9	b 30.6	a 2.6	0.053	0.748	0.5408	101	267	$\bar{0}$.7827	$\bar{0}$.9830	$\bar{0}$.8832	1.45	0.11
20	1392	T.F.	a 24.0	b 6.4	c 44.8	0.929	0.744	0.0352	106	102	$\bar{0}$.6592	$\bar{0}$.8343	$\bar{0}$.9644	0.98	0.59
20	1409	T.F.	c 30.1	b 16.6	a 25.9	0.556	0.345	$\bar{0}$.5319	195	216	$\bar{0}$.2774	$\bar{0}$.4533	$\bar{0}$.7303	1.00	0.35
20	1461	T.F.	a 27.5	c 11.5	b 34.3	0.730	0.434	0.7914	108	7	$\bar{0}$.8407	$\bar{0}$.5085	$\bar{0}$.0384	0.62	0.17
20	1487	T.F.	a 45.5	b 10.3	c 19.9	0.410	0.889	$\bar{0}$.4662	204	72	$\bar{0}$.8501	0.6072	$\bar{0}$.9345	1.97	0.34
20	1488	T.F.	a 28.9	c 20.4	b 25.8	0.536	0.211	$\bar{0}$.3065	194	353	$\bar{0}$.6409	$\bar{0}$.3695	$\bar{0}$.4758	1.06	0.96
20	1494	T.F.	b 34.0	c 16.2	a 25.1	0.520	0.440	0.8038	221	205	$\bar{0}$.7602	$\bar{0}$.5631	$\bar{0}$.1076		

Stack Number	Event Number	Scan-ning	Pion Energy (Mev) π^+	π^+	π^-	r	$\cos\theta$	Eulerian Angles $\cos\Theta$	ϕ (deg)	ψ (deg)	$\vec{a}\cdot\vec{b}$	$\vec{b}\cdot\vec{c}$	$\vec{a}\cdot\vec{c}$	$\Delta P/S\Delta P$	$\cos\delta/S\cos\delta$
20	1495	T.F.	a 20.9	b 17.3	c 37.1	0.768	0.100	0.2890	143	44	$\bar{0}$.0699	$\bar{0}$.6237	$\bar{0}$.7360	2.10	0.11
20	1514	T.F.	c 20.7	a 19.8	b 33.9	0.710	0.024	0.2645	243	34	$\bar{0}$.6274	$\bar{0}$.6869	$\bar{0}$.1346	0.86	0.43
20	1519	T.F.	c 32.2	a 12.0	b 31.0	0.643	0.505	0.2068	123	349	$\bar{0}$.2270	$\bar{0}$.8228	$\bar{0}$.3659	0.88	0.51
20	1520	T.F.	c 28.3	b 10.8	a 37.3	0.761	0.471	0.4597	102	218	$\bar{0}$.5850	0.0650	$\bar{0}$.8472	0.97	0.27
20	1525	T.F.	c 34.2	b 17.2	a [25.1]	0.512	0.415	0.7089	106	309	$\bar{0}$.1823	$\bar{0}$.5535	$\bar{0}$.7173		
20	1526	T.F.	b [27.6]	c 9.2	a 39.7	0.809	0.528	$\bar{0}$.0280	186	214	$\bar{0}$.8894	0.1577	$\bar{0}$.5913		0.34
20	1532	T.F.	b 33.7	c 14.5	a [25.4]	0.538	0.483	$\bar{0}$.1809	92	207	$\bar{0}$.7897	$\bar{0}$.5273	$\bar{0}$.1046		0.02
20	1544	T.F.	c 17.9	b 17.4	a 37.5	0.803	0.015	$\bar{0}$.1432	192	206	$\bar{0}$.7490	0.1549	$\bar{0}$.7702	1.12	0.77
20	1546	T.F.	b 18.6	a 17.9	c 38.1	0.796	0.020	0.8660	172	128	0.1149	$\bar{0}$.7558	$\bar{0}$.7372	0.56	0.51
20	1605	T.F.	a 41.0	b [27.6]	c 6.7	0.139	0.524	0.7236	123	64	$\bar{0}$.9388	0.3556	$\bar{0}$.6554		0.52
20	1611	T.F.	c 41.4	b 11.8	a 21.3	0.446	0.748	0.5693	152	187	0.3150	$\bar{0}$.7266	$\bar{0}$.8805	1.76	0.60
20	1625	T.F.	c 23.9	a 10.7	b [39.2]	0.828	0.409	0.6461	113	353	$\bar{0}$.6737	$\bar{0}$.8714	0.2248		0.00
20	1640	T.F.	a [47.6]	c 13.9	b 13.0	0.272	0.989	$\bar{0}$.1335	103	60	$\bar{0}$.9942	0.9782	$\bar{0}$.9946		0.70
20	1643	T.F.	c 27.9	b 2.7	a [44.4]	0.923	0.994	0.6172	101	293	$\bar{0}$.9973	0.9905	$\bar{0}$.9979		0.12
20	1646	T.F.	a 46.7	b 10.0	c 17.0	0.360	0.984	$\bar{0}$.6544	236	114	$\bar{0}$.9813	0.9422	$\bar{0}$.9889	0.43	0.47
20	1657	T.F.	b 18.7	a 11.0	c [42.1]	0.914	0.323	0.5390	90	97	0.5654	$\bar{0}$.9017	$\bar{0}$.8659		1.12
20	1667	T.F.	c 42.5	a 19.9	b 12.2	0.255	0.685	$\bar{0}$.4740	172	32	0.4766	$\bar{0}$.8199	$\bar{0}$.8937	0.69	0.60
20	1674	T.F.	c [28.0]	a 17.0	b 30.5	0.630	0.275	$\bar{0}$.9282	241	337	$\bar{0}$.4251	$\bar{0}$.7340	$\bar{0}$.3018		0.94
20	1675	T.F.	c 44.2	a 23.5	b 7.5	0.156	0.768	$\bar{0}$.6192	155	301	0.6721	$\bar{0}$.8652	$\bar{0}$.9525	0.72	0.62
20	1688	T.F.	b 30.0	a 8.4	c 37.2	0.767	0.587	0.4699	254	77	0.0508	$\bar{0}$.9206	$\bar{0}$.4370	2.20	0.74
20	1689	T.F.	c [38.3]	b 4.2	a 30.2	0.648	0.861	0.3218	108	283	0.2410	0.5522	$\bar{0}$.9421		0.01
20	1692	T.F.	b 34.7	c 10.4	a 33.3	0.662	0.586	0.0980	137	266	$\bar{0}$.3570	0.1933	$\bar{0}$.3398	3.66	0.26
20	1700	T.F.	c 23.3	b 20.3	a 29.5	0.629	0.077	0.9159	197	236	$\bar{0}$.5182	0.2821	$\bar{0}$.6740	1.81	0.54
20	1729	T.F.	c 39.6	a 27.8	b 8.8	0.180	0.407	0.1421	102	[illegible]	0.0687	$\bar{0}$.5672	$\bar{0}$.8608	2.38	0.00
20	1745	T.F.	b 29.8	a 29.4	c 14.5	0.307	0.012	$\bar{0}$.4455	236	159	$\bar{0}$.7601	0.3563	0.3353	0.71	0.68
20	1765	T.F.	c 45.2	b 18.8	a 12.6	0.256	0.778	0.4519	91	198	0.5825	$\bar{0}$.9192	$\bar{0}$.8420	0.51	0.28
20	1788	T.F.	c 14.7	b 12.2	a 48.0	0.999	0.926	$\bar{0}$.2974	215	219	$\bar{0}$.9916	0.9671	$\bar{0}$.9917	0.44	0.41
20	1800	T.F.	a 30.2	c 11.4	b [32.8]	0.687	0.486	0.7773	258	335	$\bar{0}$.8324	$\bar{0}$.3592	$\bar{0}$.2179		0.11
20	1806	T.F.	c 20.7	a 13.6	b [40.2]	0.841	0.226	$\bar{0}$.3803	113	25	$\bar{0}$.7555	$\bar{0}$.8317	0.2653		0.56
20	1835	T.F.	c 24.6	b 12.8	a 37.2	0.778	0.334	$\bar{0}$.6401	169	175	$\bar{0}$.5908	0.0354	$\bar{0}$.8271	0.37	0.21

Stack Number	Event Number	Scan-ning	Pion Energy (Mev) π^+	π^+	π^-	r	$\cos\theta$	$\cos\Theta$	Eulerian Angles ϕ (deg)	ψ (deg)	$\vec{a}\cdot\vec{b}$	$\vec{b}\cdot\vec{c}$	$\vec{a}\cdot\vec{c}$	$\Delta P/S\Delta P$	$\cos\delta/S\cos\delta$
20	1846	T.F.	b 16.1	a 13.8	c 44.5	0.933	0.105	$\bar{0}.8823$	159	42	0.6529	$\bar{0}.9074$	$\bar{0}.9108$	0.97	0.27
20	1868	T.F.	a [42.4]	b 18.3	c 13.7	0.287	0.700	$\bar{0}.8831$	146	135	$\bar{0}.8736$	0.4467	$\bar{0}.8248$		0.93
20	1870	T.F.	c 45.9	a 4.9	b 24.4	0.506	0.990	$\bar{0}.3657$	229	357	0.9791	$\bar{0}.9975$	$\bar{0}.9908$	0.54	0.22
20	1901	T.F.	b 31.6	c 17.1	a [25.4]	0.534	0.364	$\bar{0}.8531$	184	254	$\bar{0}.7036$	$\bar{0}.5080$	$\bar{0}.2538$		1.24
20	1937	T.F.	a 45.7	c 12.2	b 16.4	0.344	0.907	$\bar{0}.3476$	144	105	$\bar{0}.9625$	0.8392	$\bar{0}.9549$	1.15	0.49
20	1949	T.F.	c 33.1	b 21.7	a 20.7	0.427	0.291	0.6472	100	206	$\bar{0}.2361$	$\bar{0}.6421$	$\bar{0}.5935$	1.29	0.20
20	1956	T.F.	c 37.5	a 23.6	b 12.2	0.260	0.427	$\bar{0}.5393$	105	46	0.1617	$\bar{0}.6634$	$\bar{0}.8456$	0.88	0.56
20	2003	T.F.	c [38.8]	b 6.4	a 30.8	0.632	0.785	0.1288	250	327	0.1138	$\bar{0}.4858$	$\bar{0}.9233$		0.68
20	2005	T.F.	b 35.7	a 13.8	c 26.2	0.540	0.536	$\bar{0}.8929$	188	93	$\bar{0}.5232$	$\bar{0}.7894$	$\bar{0}.1096$	0.90	0.49
20	2006	T.F.	c 41.3	a 3.0	b 32.4	0.659	0.917	$\bar{0}.4056$	148	0	0.3550	$\bar{0}.9783$	$\bar{0}.5395$	1.14	1.15
20	2012	N.S.	a 24.4	c 15.8	b 34.5	0.720	0.229				$\bar{0}.7400$	$\bar{0}.5572$	$\bar{0}.1452$	0.85	1.45
20	2013	T.F.	c 23.9	b 11.7	a [39.5]	0.820	0.367	0.5520	144	302	$\bar{0}.6727$	0.1981	$\bar{0}.8578$		0.78
20	2014	T.F.	a 37.8	c 8.0	b 28.4	0.597	0.736	0.1314	180	69	$\bar{0}.9041$	0.0980	$\bar{0}.5135$	0.86	0.79

[ ] parenthesis around an energy indicates this energy was obtained by using the conservation of momentum.

* a star above an energy indicates an inelastic scatter. Conservation of momentum was used to determine the energy.

a, b, c indicates a counter-clockwise ordering of the pions.

REFERENCES

1. Brown, Camerini, Fowler, Muirhead, Powell, and Ritson, Nature 163, 82 (1949).
2. Rochester and Butler, Nature 160, 855 (1947).
3. James R. Peterson, The Masses of Identified Positive Heavy Mesons, UCRL-3368, April 1956.
4. Davies, Evans, Francois, Friedlander, Hillier, Iredale, Keefe, Menon, Perkins, Powell, Bøggild, Brene, Fowler, Hooper, Ortel, Scharff, Crane, Johnston, O'Ceallaigh, Anderson, Lawlor, Nevin, Alvial, Bonetti, di Corato, Dilworth, Levi Setti, Milone, Occhialini, Scarsi, Tomasini, Ceccarelli, Grilli, Merlin, Salandin, and Sechi, Nuovo Cimento Series X 2, 1063 (1955).
5. Birge, Perkins, Peterson, Stork, and Whitehead, Decay Characteristics and Masses of Positive K Mesons Produced by the Bevatron, UCRL-3429, May 1956 (to be published in Nuovo Cimento).
6. Proceedings of the Pisa Conference on Elementary Particles (1955), to be published as a supplement to Nuovo Cimento.
7. Proceedings of the 6th Annual Rochester Conference (Interscience, New York, 1956).
8. John E. Osher, π^0 Modes of Heavy-Meson and Hyperon Decay, UCRL-3449, June 1956.
9. R.H. Dalitz, Phil. Mag. 44, 1068 (1953);
   R.H. Dalitz, Phys. Rev. 94, 1046 (1954).
10. Communications with Dr. Donald Perkins and Dr. Peter Fowler from Bristol were of great help.
11. E. Fabri, Nuovo Cimento 11, 479 (1954).
12. Eisenberg, Lomon, and Rosendorff, Nuovo Cimento IV, 3 610 (1956).
13. F. J. Dyson, Phys. Rev. 99, 1037 (1955).
14. G. Takeda, Phys. Rev. 100, 440 (L) (1955).
15. Cool, Piccioni, and Clark, Phys. Rev. 103, 1082 (1956).
16. R.H. Dalitz, Proceedings of the 5th Annual Rochester Conference (Interscience, New York, 1955).

17. E. Amaldi, Proceedings of the Pisa Conference on Elementary Particles (1955) (to be published as a supplement to Nuovo Cimento).

18. Brene, Hansen, Hooper, and Scharff, Remarks on the Analysis of τ-Meson Experiments (reprint).

19. Teucher, Thirring, Winzeler, Nuovo Cimento 1, 733 (1955).

20. Winzeler, Proceedings of the Pisa Conference on Elementary Particles (1955) (to be published as a supplement to Nuovo Cimento).

21. T. Wentzel, Helv. Phys. Acta 22, 101 (1949).

22. Heiberg, Kruse, Marshall, Marshall, and Solmitz, Phys. Rev. 97, 250 (1955).

23. Kerth, Stork, Birge, Haddock, and Whitehead, Phys. Rev. 99, 641 (A) (1955).

24. S.B. Treiman and H.W. Wyd, Jr., Phys. Rev. 99, 1039 (1955).

25. T.D. Lee and J. Orear, Phys. Rev. 100, 932 (1955).

26. T.D. Lee and C.N. Yang, Phys. Rev. 102, 290 (1956).

27. T.D. Lee and C.N. Yang, Is Parity Conserved in Weak Interactions? (Preprint).

28. Barkas, Birnbaum, and Smith, "The Mass Ratio Method Applied to the Measurement of L-Meson Masses and the Energy Balance in Pion Decay" Phys. Rev. 101, 778 (1956).

29. W.H. Barkas and D.M. Young, Emulsion Tables. I. Heavy-Particle Functions, UCRL-2579 (Rev.), Sept. 1954.

30. M. Rich and R. Madey, Range-Energy Tables, UCRL-2301, March 1954.

31. See, for example O. Kempthorne, Design and Analysis of Experiments, Wiley, New York, 1952).

32. H. Goldstein, Classical Mechanics (Addison-Wesley, Cambrige, Mass., 1950), p. 107.